Journal Pre-proofs

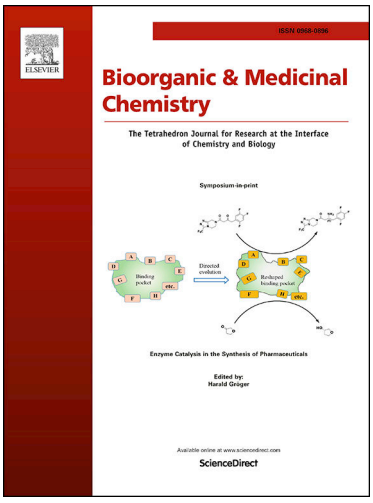

Syntheses, in vitro α-amylase and α-glucosidase dual inhibitory activities of 4-amino-1,2,4-triazole derivatives their molecular docking and kinetic studies

Emmanuel Oloruntoba Yeye, Kanwal, Khalid. Mohammed Khan, Sridevi Chigurupati, Abdul Wadood, Ashfaq Ur Rehman, Shahnaz Perveen, Mari Kannan Maharajan, Shahbaz Shamim, Shehryar Hameed, Sherifat A. Aboaba, Muhammad Taha

PII: S0968-0896(20)30281-9
DOI: https://doi.org/10.1016/j.bmc.2020.115467
Reference: BMC 115467

To appear in: *Bioorganic & Medicinal Chemistry*

Received Date: 29 December 2019
Revised Date: 20 March 2020
Accepted Date: 25 March 2020

Please cite this article as: E. Oloruntoba Yeye, Kanwal, Khalid. Mohammed Khan, S. Chigurupati, A. Wadood, A. Ur Rehman, S. Perveen, M. Kannan Maharajan, S. Shamim, S. Hameed, S.A. Aboaba, M. Taha, Syntheses, in vitro α-amylase and α-glucosidase dual inhibitory activities of 4-amino-1,2,4-triazole derivatives their molecular docking and kinetic studies, *Bioorganic & Medicinal Chemistry* (2020), doi: https://doi.org/10.1016/j.bmc.2020.115467

Syntheses, *in vitro* α-amylase and α-glucosidase dual inhibitory activities of 4-amino-1,2,4-triazole derivatives their molecular docking and kinetic studies

Emmanuel Oloruntoba Yeye,[a,b] Kanwal,[a] Khalid. Mohammed Khan,[*a,c] Sridevi Chigurupati,[d] Abdul Wadood,[e] Ashfaq Ur Rehman,[e] Shahnaz Perveen,[f] Mari Kannan Maharajan,[g] Shahbaz Shamim,[a] Shehryar Hameed,[a] Sherifat A. Aboaba,[b] Muhammad Taha[c]

[a]*H. E. J. Research Institute of Chemistry, International Center for Chemical and Biological Sciences, University of Karachi, Karachi-75270, Pakistan*
[b]*Organic Unit, Chemistry Department, University of Ibadan, Nigeria*
[c]*Department of Clinical Pharmacy, Institute for Research and Medical Consultations (IRMC), Imam Abdulrahman Bin Faisal University, P.O. Box 1982, Dammam 31441, Saudi Arabia*
[d]*Department of Medicinal Chemistry and Pharmacognosy, Faculty of Pharmacy, Qassim University, Buraidah 52571, Kingdom of Saudi Arabia*
[e]*Department of Biochemistry, Computational Medicinal Chemistry Laboratory, UCSS, Abdul Wali Khan University, Mardan, Pakistan*
[f]*PCSIR Laboratories Complex, Karachi, Shahra-e-Dr. Salimuzzaman Siddiqui, Karachi-75280, Pakistan*
[g]*School of Pharmacy, International Medical University, Kuala Lumpur, 57000, Malaysia*

Abstract: Thirty-three 4-amino-1,2,4-triazole derivatives **1-33** were synthesized by reacting 4-amino-1,2,4-triazole with a variety of benzaldehydes. The synthetic molecules were characterized *via* ^{1}H-NMR and EI-MS spectroscopic techniques and evaluated for their anti-hyperglycemic potential. Compounds **1-33** exhibited good to moderate *in vitro* α-amylase and α-glucosidase inhibitory activities in the range of IC_{50} values 2.01 ± 0.03 - 6.44 ± 0.16 and 2.09 ± 0.08 - 6.54 ± 0.10 μM as compared to the standard acarbose (IC_{50} = 1.92 ± 0.17 μM) and (IC_{50} = 1.99 ± 0.07 μM), respectively. The limited structure-activity relationship suggested that different substitutions on aryl part of the synthetic compounds are responsible for variable activity. Kinetic study predicted that compounds **1-33** followed mixed and non-competitive type of inhibitions against α-amylase and α-glucosidase enzymes, respectively. *In silico* studies revealed that both triazole and aryl ring along with different substitutions were playing an important role in the binding interactions of inhibitors within the enzyme pocket. The synthetic molecules were found to have dual inhibitory potential against both enzymes thus they may serve as lead candidates for the drug development and research in the future studies.

*Corresponding Authors: khalid.khan@iccs.edu; drkhalidhej@gmail.com, Tel.: +922134824910, Fax: +922134819018

Introduction:

Triazoles belongs to the nitrogen containing heterocyclic compounds and are comprised of a five-membered ring system with two carbon and three nitrogen atoms in the ring having alternate *π*-bonds [1]. It exists in two isomeric forms, 1,2,3-triazole and 1,2,4-triazole. Triazoles are pharmacologically active molecules due to their structural properties, like moderate dipole character, hydrogen bonding capability, ion-dipole, π-π stacking, cation-π, hydrophobic effect, van der Waal forces, rigidity, and stability. These characteristic structural features make them more stable under *in vivo* conditions which lead to their superior pharmacological activities [2-5]. Enzyme inhibition studies remain an important area of pharmacology. The activity of natural substrates towards their respective enzymes have been blocked or altered by the action of enzyme inhibitors [6]. These enzyme inhibitors suppress the over-expression of an enzyme thus preventing different disorders. Therefore, the search of new and potential enzyme inhibitors has attracted the considerable attention of medicinal chemists. 1,2,4-Triazoles and their derivatives has been widely known for their synthetic and biological importance [7] and this ring system is also a part of wide variety of therapeutically important drug candidates [8] (Figure-1).

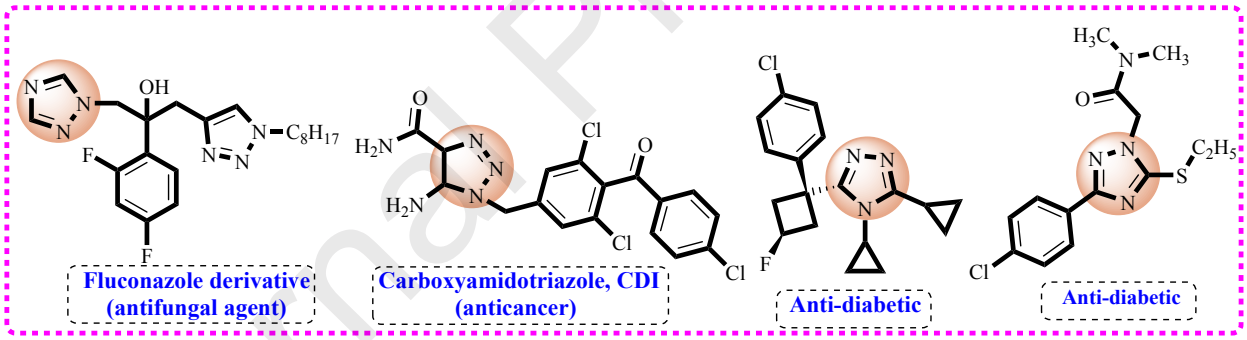

Figure-1: 1,2,4-triazole containing drugs and their bioactivities

Diabetes mellitus is amongst the most prevailing chronic metabolic disorders and is usually characterized by hyperglycemia which is caused due to less insulin action or secretion or both. The chronic hyperglycemia is associated with microvascular complications thus causing the eyes, kidneys, and nerves, as well as it leads to an increased risk for cardiovascular disease (CVD) [9]. *α*-Glucosidase belongs to the family of hydrolase enzyme and is found in small intestine. It hydrolyses carbohydrates to glucose during digestion which is then absorbed into blood stream. The excess amount of glucose in the blood increases postprandial blood glucose level thus leads to diabetes. Therefore, to control the postprandial hyperglycemia in type-II- diabetes mellitus, the

activity of enzyme should be suppressed by using different inhibitors [10-16]. Several *α*-glucosidase inhibitors such as miglitol, voglibose, and acarbose have been reported in the literature and are used to decrease the postprandial blood glucose levels [17-18]. *α*-Amylase (EC 3.2.1.1) is another enzyme of hydrolase family bearing calcium atom as a metal co-factor. It catalyzes the hydrolysis of polysaccharides to monosaccharides [19]. The absoprtion of starch in human body is catalyzed by the hydrolytic action of *α*-amylase and *α*-glucosidase enzymes [20]. Hence, the development of potent *α*-amylase inhibitors that can be used as chemotherapeutic agents might be a better approach for the treatment of diabetes [19,21].

Since our research group had already reported the diverse biological activities of compounds derived from 1,2,4-triazoles [22-28], therefore, in continuation of our previous work we had selected and modified another compound from this class in order to explore its potential. It is worth-noting that our research group has reported various classes of compounds including benzotriazoles, pyrazolones, and other heterocyclic molecules as dual and potential inhibitors of *α*-amylase and *α*-glucosidase enzymes. In the current study 1,2,4-triazole derivatives **1-33** were synthesized and subjected for their *α*-amylase and *α*-glucosidase inhibitory activities and the results showed that these compounds were found to exhibit potential inhibitory activities against both enzymes and may act as lead molecules (Figure-2). To the best of our knowledge compounds **1**, **5-7**, **10-12**, **13**, **17**, **19-23**, **25-28**, and **32** are new while others are already reported.

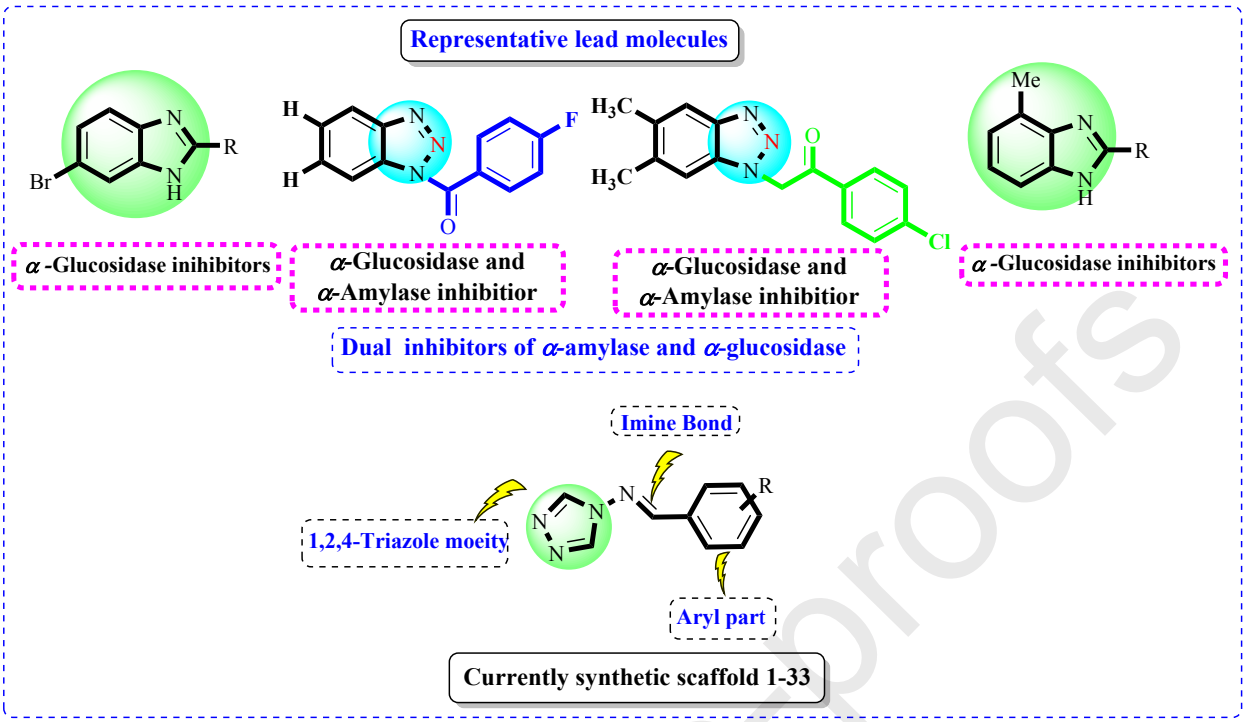

Figure-2: Rational of the current study.

Results and Discussion

Chemistry

Schiff base derivatives of 4-amino-1,2,4-triazole **1-33** were synthesized by refluxing 4-amino-1,2,4-triazole with different substituted benzaldehydes in equimolar proportion in ethanol. H_2SO_4 was added in catalytic amount and reaction was refluxed for 2-4 h. The reaction progress was periodically observed by thin layer chromatography (TLC). After completion of reaction, the solvent was evaporated on a rotary evaporator. Further purifications of synthetic molecules was done by the crystallization from ethanol (Scheme-1). Spectroscopic techniques EI-MS and ^{1}H-NMR were used to elucidate the structures of synthetic compounds.

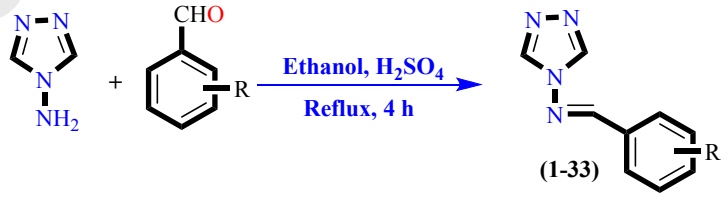

Scheme-1: Synthesis of Schiff base derivatives of 4-amino-1,2,4-triazole **1-33**.

In vitro α-amylase and α-glucosidase activities:

The synthetic derivatives **1-33** displayed good α-amylase and α-glucosidase inhibitory activities, having IC_{50} values in the range of 2.01 ± 0.03 – 6.44 ± 0.16 μM and 2.09 ± 0.08 – 6.54 ± 0.10 μM

as compared to the standard acarbose (IC_{50} = 1.92 ± 0.17) and (IC_{50} = 1.99 ± 0.07 μM), respectively. Generally, the synthetic molecules were comprised of 1,2,4-triazole ring, aryl ring, and imine bond. However, the aryl ring had different substitutions ‘‘R” which apparently played their role in the inhibitory potential of compounds and variations in the inhibitory activities are attributed to the type of substitutions and their respective positions on the aryl part (Table-1) (Figure-3).

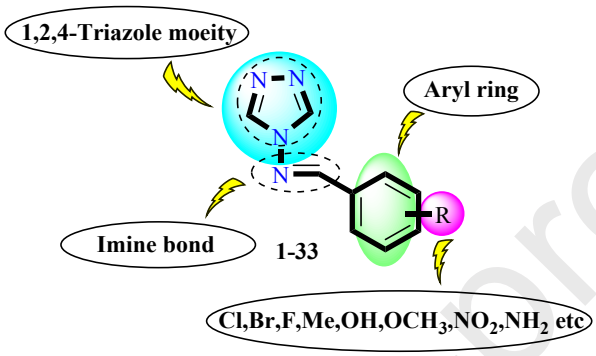

Figure-3: General structure of synthetic compounds

Table-1: *In vitro* α-amylase and α-glucosidase inhibition of Schiff base derivatives of 4-amino-1,2,4-triazole (**1-33**)

Compound No.	Structures	α-Amylase inhibition IC_{50} ± SEM[a] (μM)	α-Glucosidase Inhibition IC_{50} ± SEM[a] (μM)
1	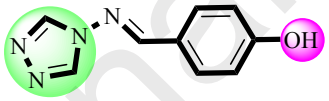	2.99 ± 0.13	2.62 ± 0.08
2	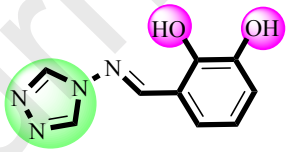	5.69 ± 0.1	5.44 ± 0.11
3	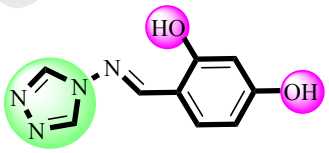	5.95 ± 0.07	5.44 ± 0.07
4	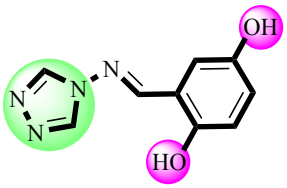	5.27 ± 0.11	5.37 ± 0.11

5	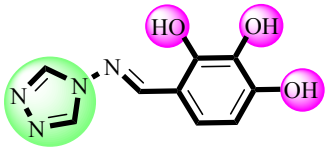	5.92 ± 0.15	5.74 ± 0.05
6	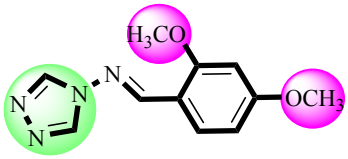	4.37 ± 0.02	4.28 ± 0.08
7	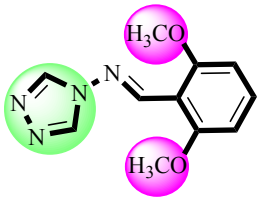	4.37 ± 0.11	4.29 ± 0.1
8	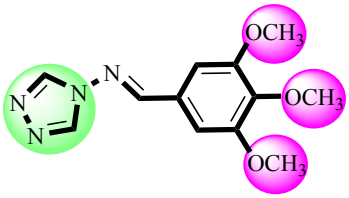	5.12 ± 0.08	5.46 ± 0.1
9	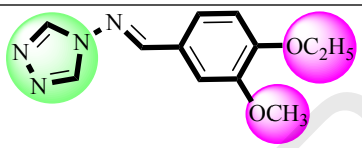	5.24 ± 0.05	5.36 ± 0.1
10	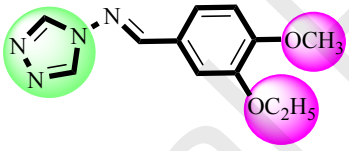	5.22 ± 0.07	5.47 ± 0.11
11	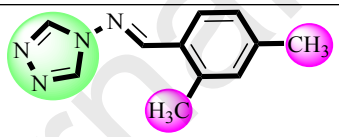	4.34 ± 0.06	4.27 ± 0.16
12	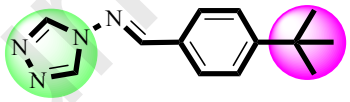	6.44 ± 0.16	6.37 ± 0.02
13	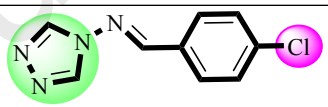	4.36 ± 0.1	4.28 ± 0.03
14	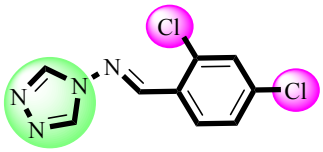	2.18 ± 0.12	2.49 ± 0.05
15	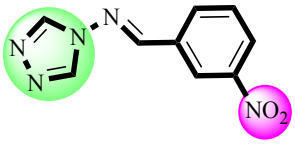	5.97 ± 0.08	5.37 ± 0.08

16	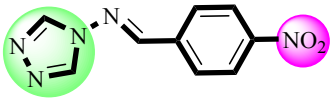	2.36 ± 0.1	2.47 ± 0.11
17	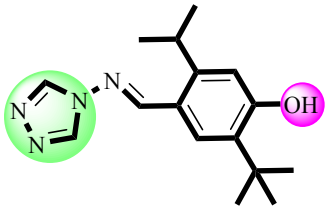	6.23 ± 0.09	6.34 ± 0.06
18	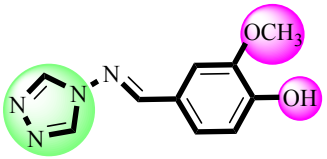	5.94 ± 0.07	5.3 ± 0.14
19	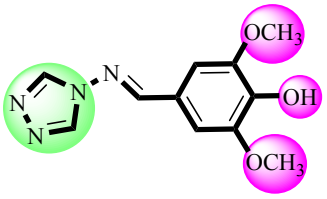	3.31 ± 0.08	3.27 ± 0.01
20	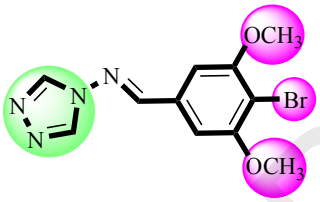	2.25 ± 1.05	2.52 ± 0.09
21	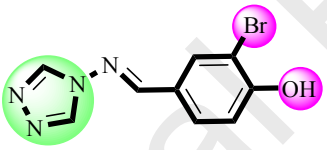	2.27 ± 0.01	2.37 ± 0.02
22	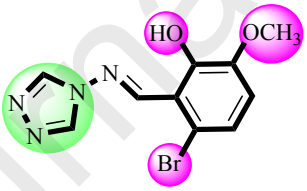	5.25 ± 1.05	5.52 ± 0.09
23	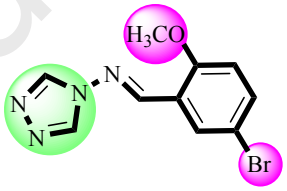	3.3 ± 0.04	3.46 ± 0.09
24	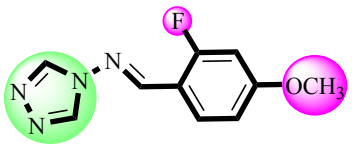	2.9 ± 0.04	2.33 ± 0.13

25	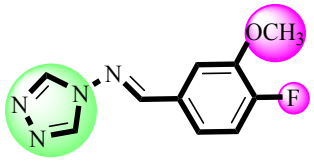	2.33 ± 0.13	2.27 ± 0.11
26	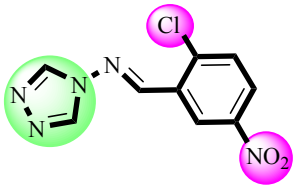	4.46 ± 0.09	4.37 ± 0.11
27	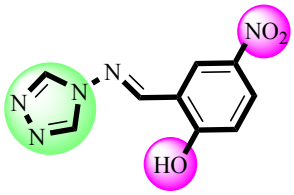	2.41 ± 0.09	2.31 ± 0.07
28	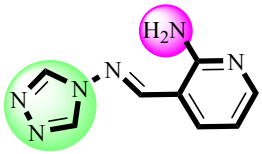	2.28 ± 0.08	2.44 ± 0.03
29	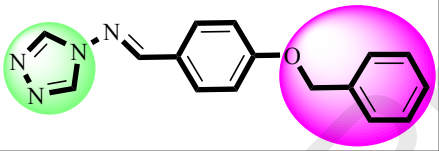	5.04 ± 0.3	5.44 ± 0.29
30	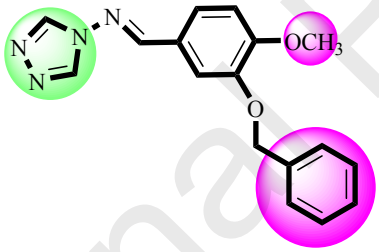	6.23 ± 0.1	6.54 ± 0.10
31	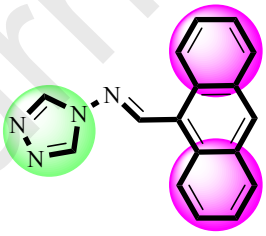	5.27 ± 0.16	5.41 ± 0.03
32	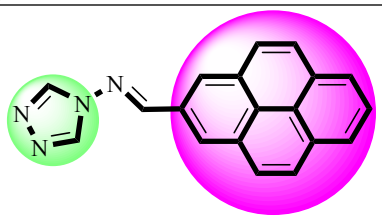	6.41 ± 0.03	6.3 ± 0.04

33	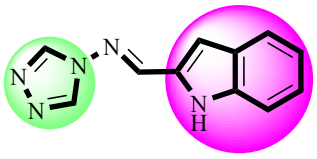	2.01 ± 0.03	2.09 ± 0.08
Standard[b] = Acarbose		1.92 ± 0.17	1.99 ± 0.07

IC_{50} SEM[a] = Mean ± Standard error of mean; Standard[b] = Inhibitor for *α*-amylase, *α*-glucosidase inhibitory activity

Structure-activity relationship (SAR) for *α*-amylase and *α*-glucosidase inhibitory activities

All structural features such as, triazole moiety, imine bond, and different substituted aryl parts are equally playing their role in the *α*-amylase and *α*-glucosidase inhibition. Nonetheless, different chemical entities on aryl ring resulted in variable activity of the synthetic molecules. Based on variable substitutions and their different positions and numbers on aryl ring a limited structure-activity relationship was rationalized. However, all synthetic compounds were found to be dual inhibitors of *α*-amylase and *α*-glucosidase.

Compounds **1-5** having variable numbers and positions of hydroxy substituents have displayed good inhibitory activities against *α*-amylase and *α*-glucosidase enzymes, respectively. Among them, compound **1** (IC_{50} = 2.99 ± 0.13 *μ*M) (IC_{50} = 2.62 ± 0.08 *μ*M) with *para* hydroxy substitution was more active as compared to other derivatives. Compound **2** (IC_{50} = 5.69 ± 0.1 *μ*M) (IC_{50} = 5.44 ± 0.11 *μ*M) having two hydroxy groups at *meta* and *para* positions of aryl ring was found to be two folds less active in comparison with compound **1**. Compound **3** (IC_{50} = 5.95 ± 0.07 *μ*M) (IC_{50} = 5.44 ± 0.07 *μ*M) with *ortho*, *para* hydroxy substitution displayed decreased *α*-amylase activity, however, *α*-glucosidase inhibition was similar to compound **2**. Another dihydroxy substituted compound **4** (IC_{50} = 5.27 ± 0.11 *μ*M), (IC_{50} = 5.37 ± 0.11 *μ*M) with hydroxy substituents *para* to each other showed good activity as compared to its structurally similar compounds **2** and **3**. The trihydroxy substituted compound **5** (IC_{50} = 5.92 ± 0.15 *μ*M), (IC_{50} = 5.74 ± 0.05 *μ*M) with three hydroxy groups adjacent to each other exhibited comparable *α*-amylase activity to compound **3**, however, it was less active against *α*-glucosidase enzyme. Thus it can be observed that substitution of hydroxy group at different positions of aryl ring was responsible for variable activity of synthetic molecules, might be the change in positions alter the binding interaction of molecules within the active site of enzyme. The different numbers of hydroxy groups are also found to be responsible for the variable activity, with increasing the number of hydroxy groups on aryl ring a sharp change in activity was observed (Figure-4).

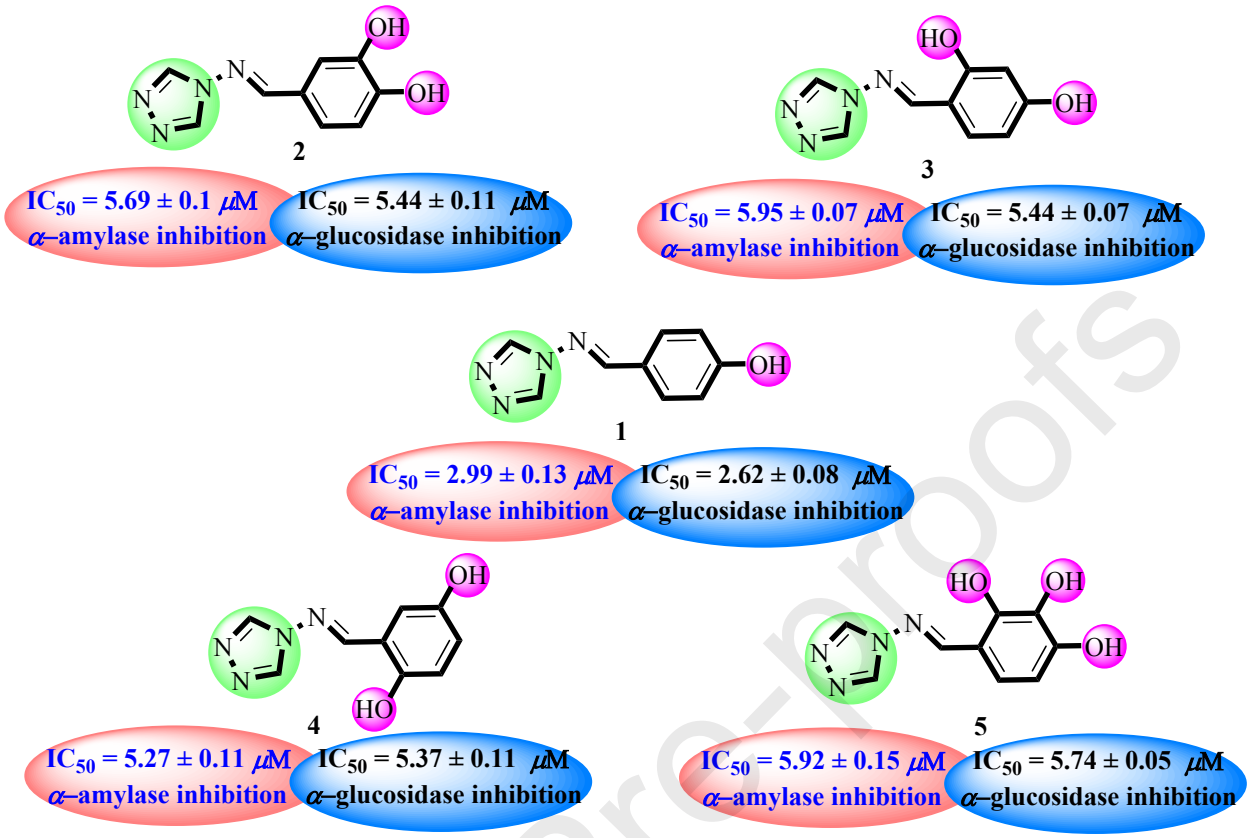

Figure-4: Structure-activity relationship of compounds 1-5

The methoxy substituted compounds **6-10** also displayed variable activity and were found to be less active in comparison with hydroxy substituted compounds. Compound **6** (IC_{50} = 4.37 ± 0.02 μM), (IC_{50} = 4.28 ± 0.08 μM) with *ortho* and *para* methoxy substituents displayed similar activity with its positional isomer **7** (IC_{50} = 4.37 ± 0.11 μM), (IC_{50} = 4.29 ± 0.1 μM) having both methoxy groups at *ortho* positions. The activity was decreased with an addition of methoxy group on the aryl ring in compound **8** (IC_{50} = 5.12 ± 0.08 μM), (IC_{50} = 5.46 ± 0.1 μM). Compounds **9** (IC_{50} = 5.24 ± 0.05 μM), (IC_{50} = 5.36 ± 0.1 μM) and **10** (IC_{50} = 5.22 ± 0.07 μM), (IC_{50} = 5.47 ± 0.11 μM) were positional isomers of each other and bear methoxy and ethoxy groups. These compounds displayed comparable α-amylase activity with each other, nevertheless, slight variation in the α-glucosidase activity might be due to the changed positions of methoxy and ethoxy groups. Thus, it showed that increasing the number of substituents or replacing those with bulkier groups resulted in decreased inhibition due to which the molecules might not able to interact effectively within the active pocket of enzyme (Figure-5).

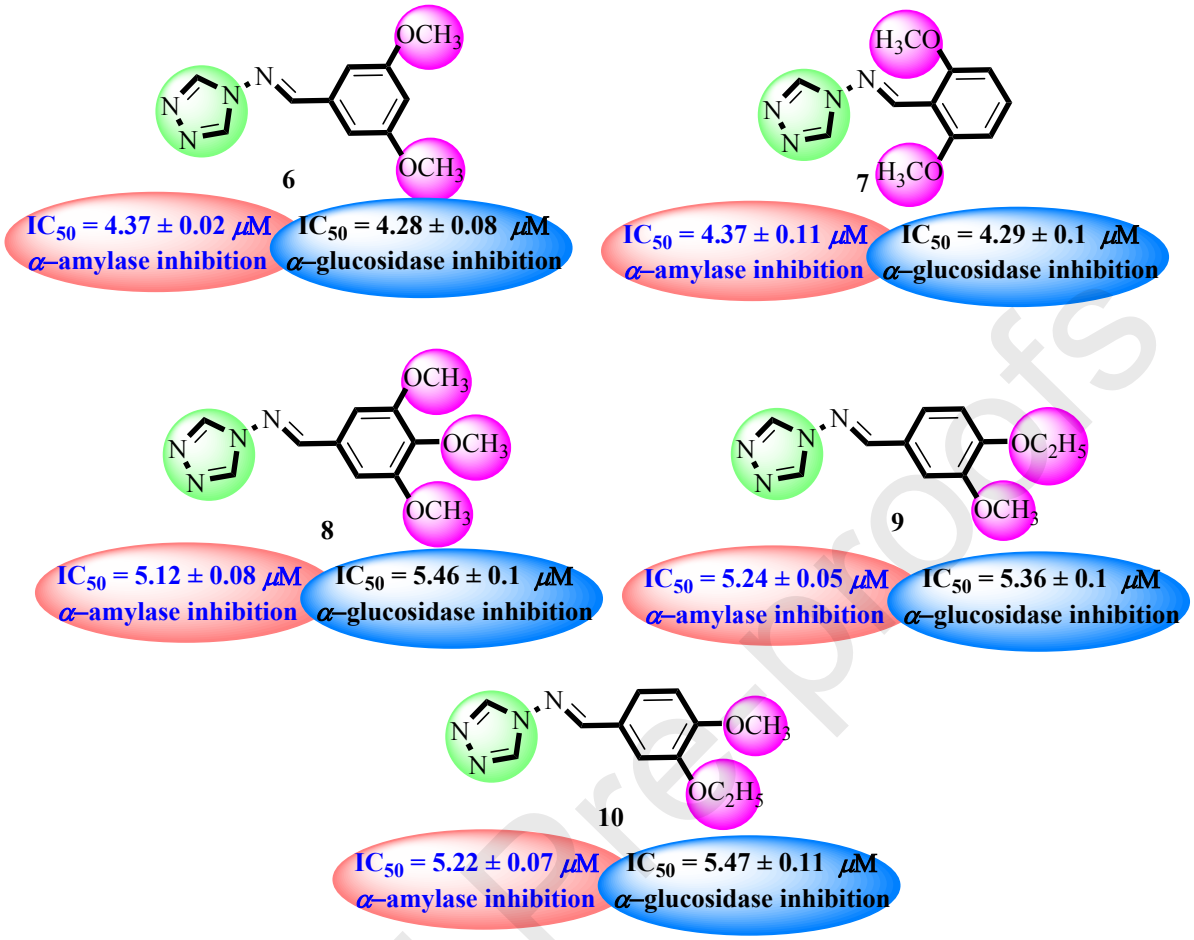

Figure-5: Structure-activity relationship of compounds 6-10

Compounds **11** and **12** with different alkyl substituents were also found to have moderate activity but they were less active in comparison with hydroxy and methoxy substituted compounds. Amongst them, compound **11** (IC_{50} = 4.34 ± 0.06 μM), (IC_{50} = 4.27 ± 0.06 μM) with two methyl substituents *meta* to each other displayed good inhibition in comparison with compound **12** (IC_{50} = 6.44 ± 0.16 μM), (IC_{50} = 6.37 ± 0.02 μM) having *para* substituted *t*-butyl group. This pattern again showed that the compounds with bulkier substituents are less active. Amongst halogen substituted analogs **13-14**, compound **13** (IC_{50} = 4.36 ± 0.10 μM) (IC_{50} = 4.28 ± 0.03 μM) with *para* chloro substitution displayed moderate inhibition against both enzymes. Nevertheless, compound **14** (IC_{50} = 2.18 ± 0.11 μM), (IC_{50} = 2.49 ± 0.05 μM) with dichloro substituents at *ortho* and *para* positions displayed potential inhibition as compared to compound **13** and was found to be second most active molecule of the series (Figure-6).

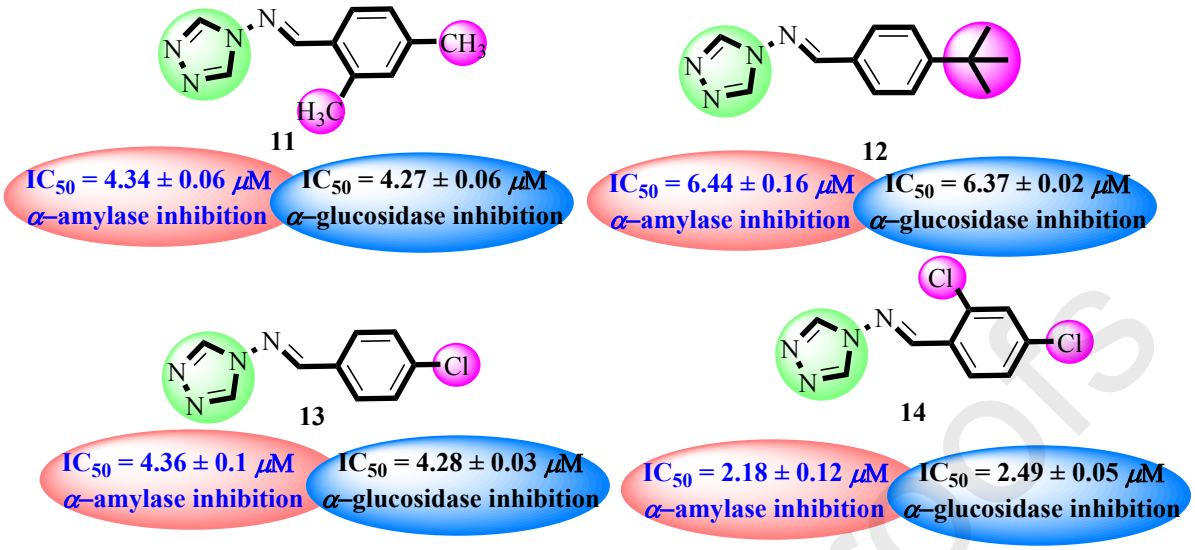

Figure-6: Structure-activity relationship of compounds 11-15

The nitro substituted compounds **15** (IC_{50} = 5.97 ± 0.08 μM), (IC_{50} = 5.37 ± 0.08 μM) and **16** (IC_{50} = 2.36 ± 0.10 μM), (IC_{50} = 2.47 ± 0.11 μM) bearing nitro groups at *meta* and *para* positions, respectively, displayed variable inhibition. A sharp change in activity of compound **16** was observed and it might be attributed to the *para* position of nitro group. The addition of chloro at *ortho* position along with nitro group resulted in increased inhibition as in compound **26** (IC_{50} = 4.46 ± 0.09 μM) (IC_{50} = 4.37 ± 0.09 μM) as compared to compound **15** bearing *meta* substituted nitro group. Compound **27** (IC_{50} = 2.41 ± 0.09 μM) (IC_{50} = 2.31 ± 0.09 μM) with combination of hydroxy and nitro groups *meta* to each other also displayed increased potential in comparison with compounds **15** and **26**. However, all these compounds were less active in comparison with compound **16** which demonstrated that substitution of nitro group at *para* position favors the binding interactions of enzyme with the molecule (Figure-7).

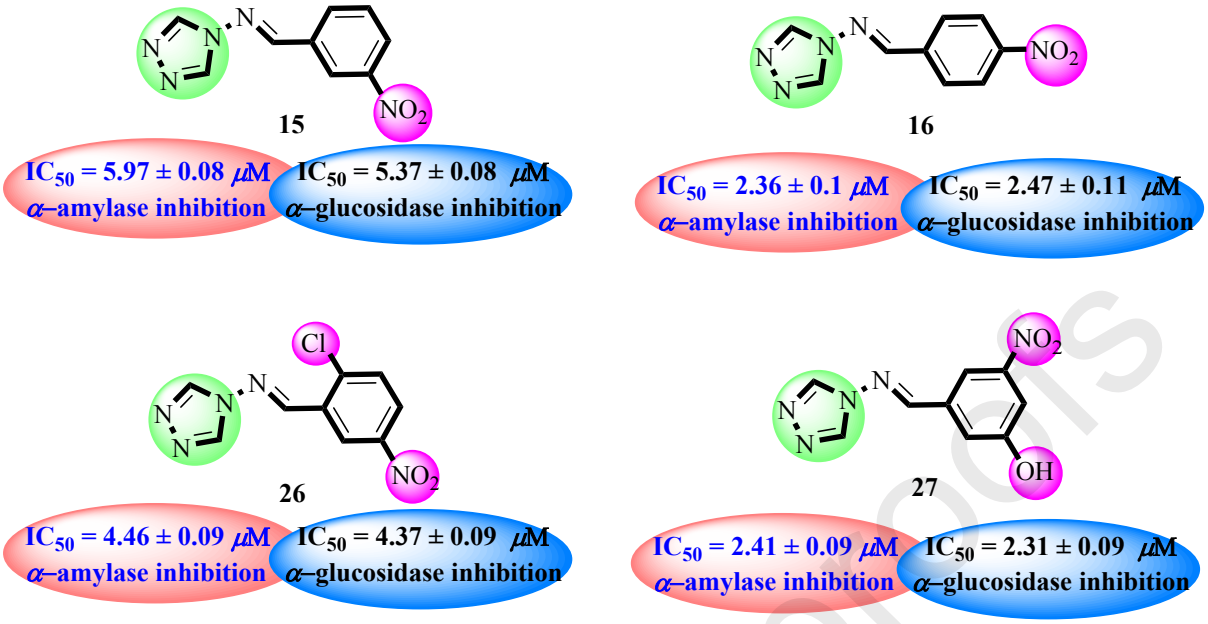

Figure-7: Structure-activity relationship of compounds 15-16 and 26-27

Compounds **17-25** having mixed substitution of hydroxy, methoxy, and halogens, displayed variable activities according to the nature and position of substituents. Amongst them, compound **17** (IC_{50} = 6.32 ± 0.09 μM) (IC_{50} = 6.34 ± 0.06 μM) with *para* hydroxy, and two *t*-butyl groups *para* to each other was less active might be the presence of two bulky groups resulted in the increased steric hindrance. However, combination of hydroxy and methoxy substituents in compound **18** (IC_{50} = 5.94 ± 0.07 μM) (IC_{50} = 5.3 ± 0.14 μM) at *para* and *meta* positions, respectively, displayed good activity. Interestingly, addition of another methoxy group *ortho* to hydroxy in compound **19** (IC_{50} = 3.31 ± 0.08 μM) (IC_{50} = 3.27 ± 0.01 μM) resulted in increased inhibition as compared to compound **18**. Replacement of hydroxy group with bromo in compound **20** (IC_{50} = 2.25 ± 1.05 μM) (IC_{50} = 2.52 ± 1.05 μM) displayed further increased activity. However, compound **21** (IC_{50} = 2.27 ± 0.01 μM) (IC_{50} = 2.37 ± 0.01 μM) with bromo and hydroxy groups *ortho* to each other displayed superior activity in comparison with compounds **17-21**, it showed that bromo and hydroxy groups are actively participating in the activity. Nevertheless, changing the position of bromo and hydroxy substituents and addition of methoxy group on aryl ring resulted in decreased activity in compound **22** (IC_{50} = 5.25 ± 1.05 μM) (IC_{50} = 5.52 ± 0.09 μM). Compound **23** (IC_{50} = 3.30 ± 0.04 μM) (IC_{50} = 3.46 ± 0.09 μM) with bromo and methoxy groups *para* with respect to each other was less active as compared to compounds **24** (IC_{50} = 2.90 ± 0.04 μM) (IC_{50} = 2.33 ± 0.13 μM) and **25** (IC_{50} = 2.33 ± 0.13 μM) (IC_{50} = 2.27 ± 0.11 μM) with combination of methoxy and fluorine. The above results revealed that combination of fluoro with methoxy and

bromo with hydroxy have displayed potential inhibition, however, slight variations in activity of these compounds was due to different positions of methoxy, bromo, and fluoro groups (Figure-8).

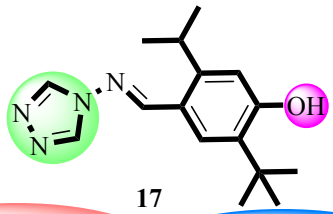

17

IC_{50} = 6.23 ± 0.09 μM α–amylase inhibition

IC_{50} = 6.34 ± 0.06 μM α–glucosidase inhibition

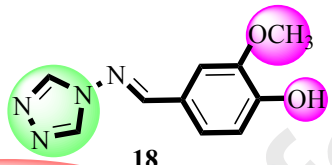

18

IC_{50} = 5.94 ± 0.07 μM α–amylase inhibition

IC_{50} = 5.3 ± 0.14 μM α–glucosidase inhibition

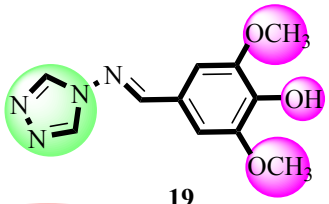

19

IC_{50} = 3.31 ± 0.08 μM α–amylase inhibition

IC_{50} = 3.27 ± 0.01 μM α–glucosidase inhibition

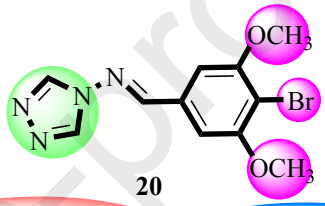

20

IC_{50} = 2.25 ± 1.05 μM α–amylase inhibition

IC_{50} = 2.52 ± 1.05 μM α–glucosidase inhibition

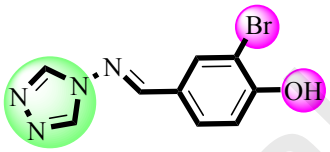

21

IC_{50} = 2.27 ± 0.01 μM α–amylase inhibition

IC_{50} = 2.37 ± 0.01 μM α–glucosidase inhibition

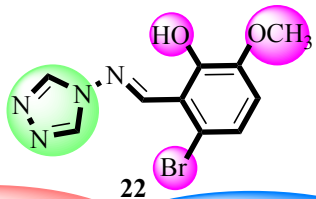

22

IC_{50} = 5.25 ± 1.05 μM α–amylase inhibition

IC_{50} = 5.52 ± 0.09 μM α–glucosidase inhibition

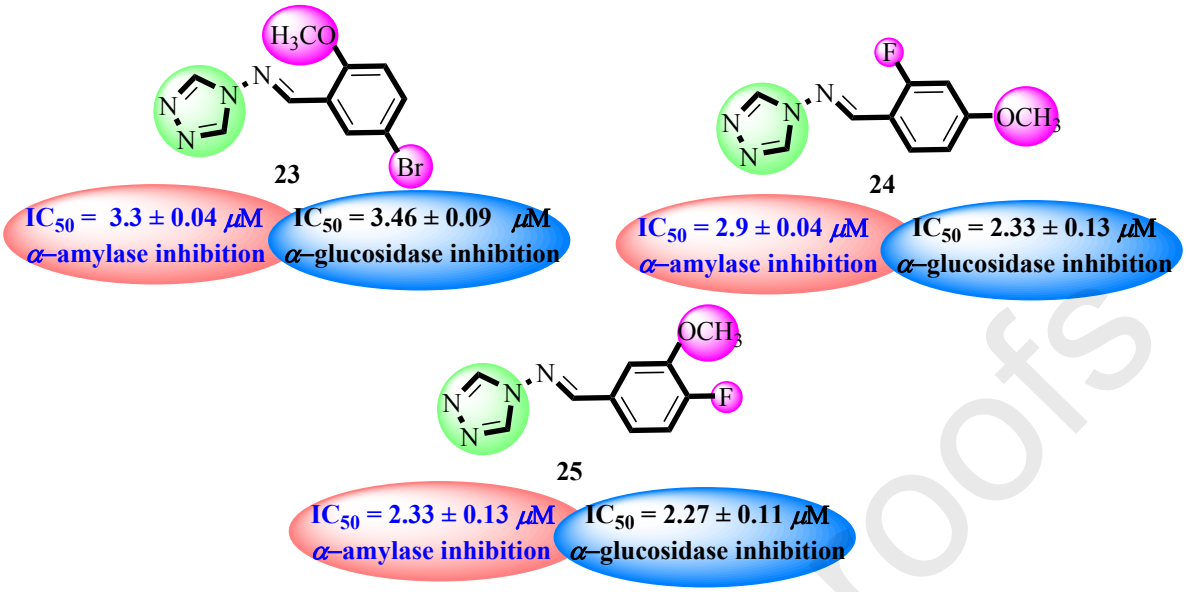

Figure-8: Structure-activity relationship of compounds 17-25

Compounds **28-33** bear different aryl rings including heterocyclic rings and bulky conjugated ring systems therefore, these molecules displayed quite variable results. Compound **28** (IC_{50} = 2.28 ± 0.08 μM) (IC_{50} = 2.44 ± 0.03 μM) bearing 2-amino pyridine ring exhibited good inhibition against both enzymes. However, compound **29** (IC_{50} = 5.04 ± 0.3 μM) (IC_{50} = 5.44 ± 0.29 μM) with benzyloxy group at the aryl part was less active might be the incorporation of bulky group make it more difficult to interact within the active site of enzyme. Addition of methoxy group along with benzyloxy group resulted in further declined activity in compound **30** (IC_{50} = 6.23 ± 0.1 μM) (IC_{50} = 6.54 ± 0.10 μM). Compounds **31** (IC_{50} = 5.27 ± 0.16 μM) (IC_{50} = 5.41 ± 0.03 μM) and **32** (IC_{50} = 6.41 ± 0.03 μM) (IC_{50} = 6.3 ± 0.04 μM) with anthracene and pyrene rings, respectively, also showed weak inhibition which showed that bulky groups are creating a steric hindrance thus the molecules are unable to interact within the active site of enzyme. Compound **33** (IC_{50} = 2.01 ± 0.03 μM) (IC_{50} = 2.09 ± 0.08 μM) having indole ring as aryl part was most active molecule of the series and displayed good inhibition as compared to the standard acarbose, might be the pyrrole ring of indole is capable of forming the binding interactions with the active site of enzyme (Figure-9).

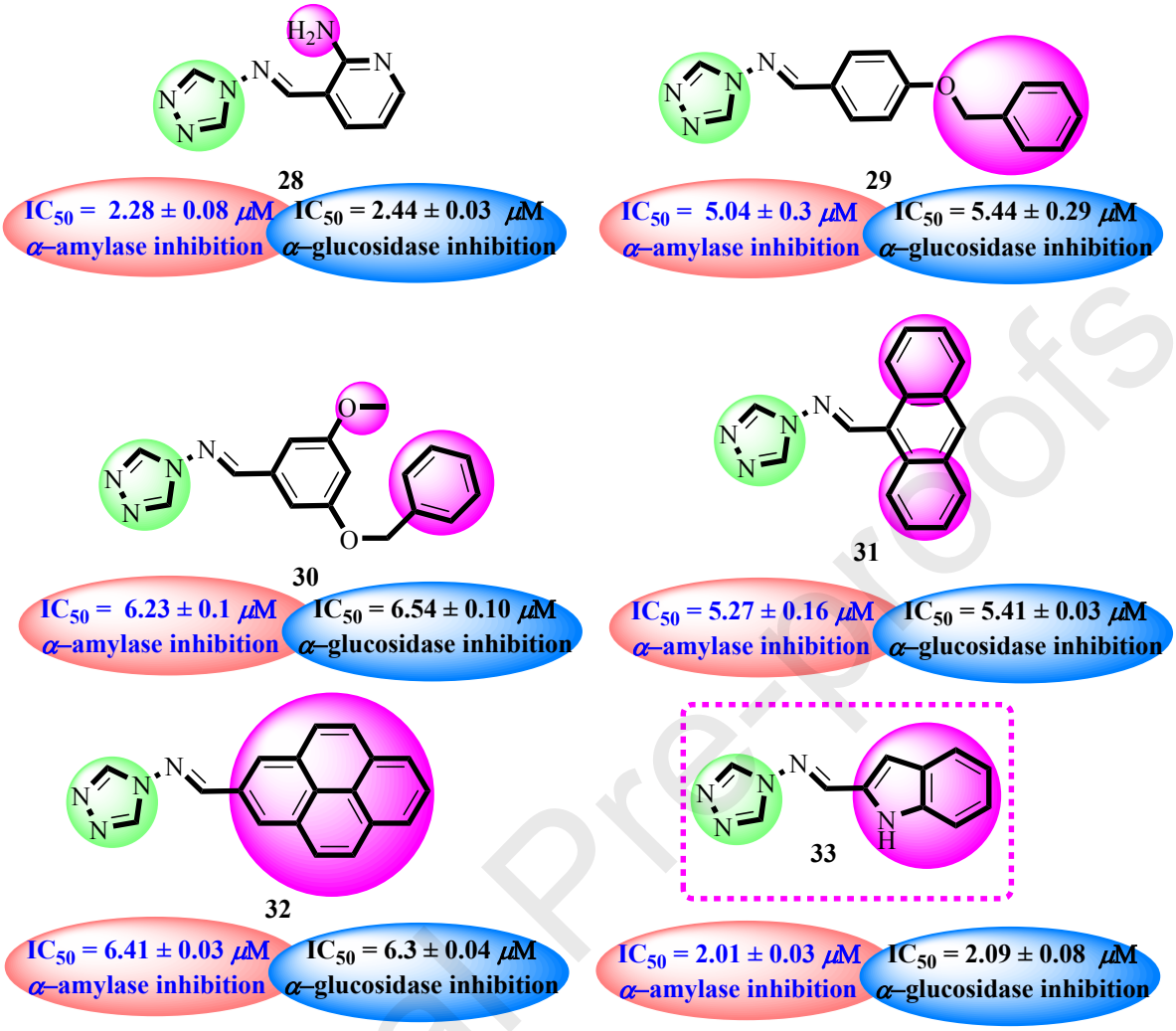

Figure-9: Structure-activity relationship of compounds 29-33

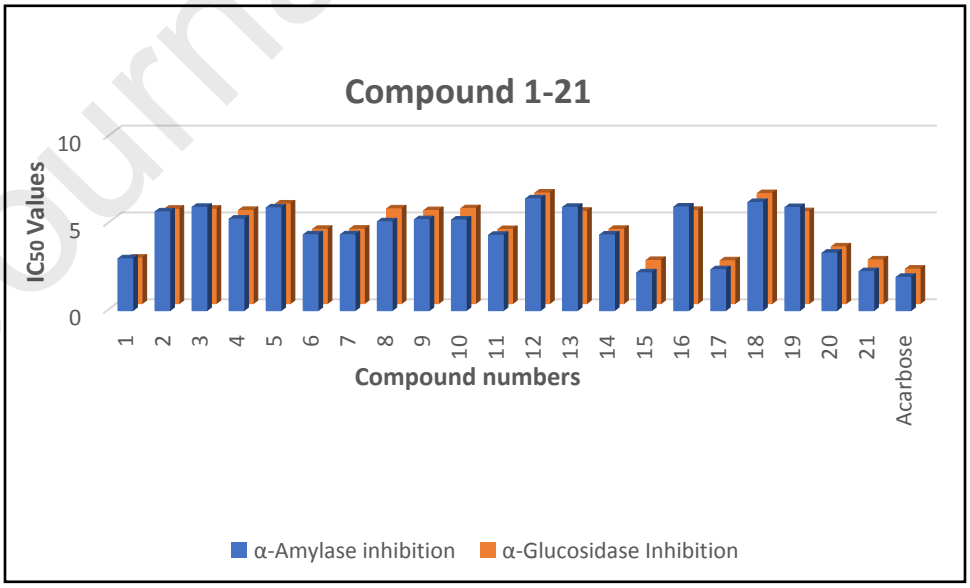

Figure-11: Comparison of α-amylase and α-glucosidase activities of compound **1-21**

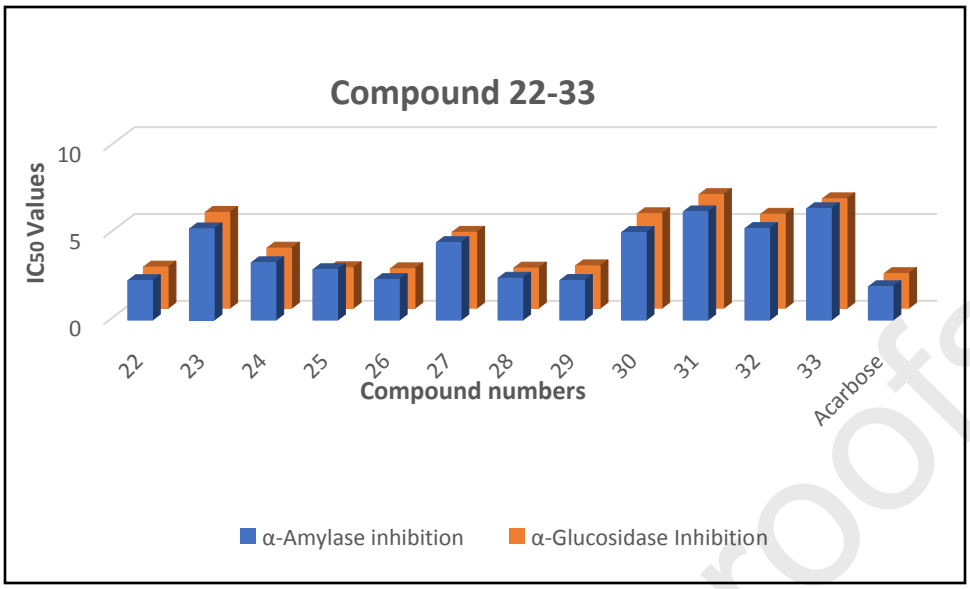

Figure-12: Comparison of *α*-amylase and *α*-glucosidase activities of compound **22-33**

Kinetic characterization of *α*-amylase inhibition

Kinetic studies on the most active *α*-amylase inhibitors **1**, **14**, **16**, **20**, **21**, **24**, **25**, **27**, **28**, and **33** were carried out to interpret the inhibition mechanism of these compounds. The enzyme inhibition mechanism analyzed by using Sigma-Plot enzyme kinetic software through various parameters as shown in Figure-13 and Table-2. The kinetic studies revealed that the synthetic compounds showed mixed type of inhibition.

Table-2: Kinetic studies of active compounds for *α*-amylase inhibition

S. No	Compound. No	Vmax (µM/min)[1]	Km (mM)	AICc	R^2	Type of inhibition
1	**1**	237.4	1.3	110.6	0.912	Mixed type
2	**14**	220.8	1.2	108.3	0.915	Mixed type
3	**16**	206.8	0.9	106.4	0.902	Mixed type
4	**20**	241.5	1.3	110.2	0.935	Mixed type
5	**21**	220.8	1.2	112.3	0.905	Mixed type
6	**24**	237.7	1.3	108.3	0.922	Mixed type
7	**25**	240.8	1.3	108.4	0.923	Mixed type
8	**27**	231.9	1.3	110.3	0.905	Mixed type
9	**28**	212.7	1.0	118.2	0.975	Mixed type
10	**33**	256.1	1.5	121.7	0.992	Mixed type

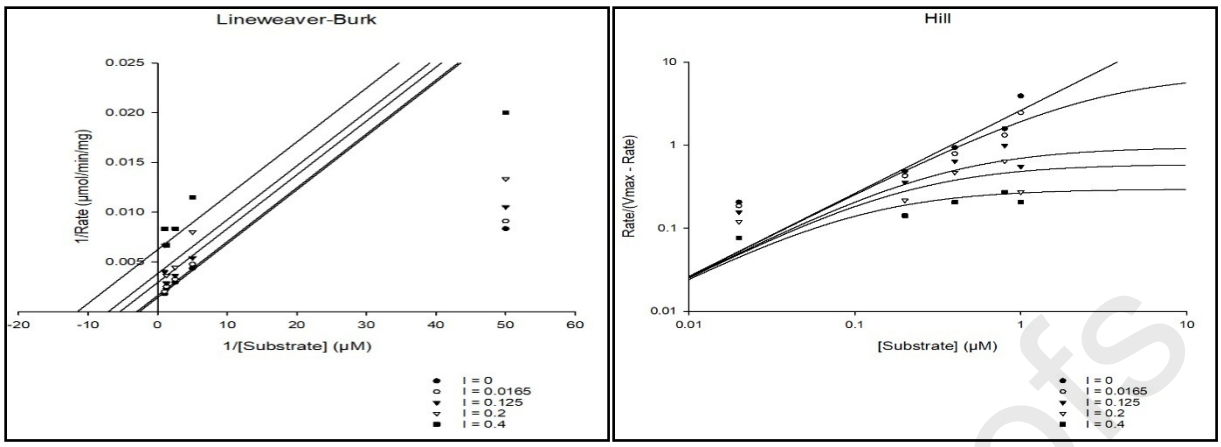

Figure-13:A) Lineweaver-Burk plot of 1/[S] Vs 1/Rate in the different concentration of mixed-type inhibitor. **B)** Hill plot of different concentration of [S] Vs Rate (Vmax-Rate) in the different concentration of mixed-type inhibitor.

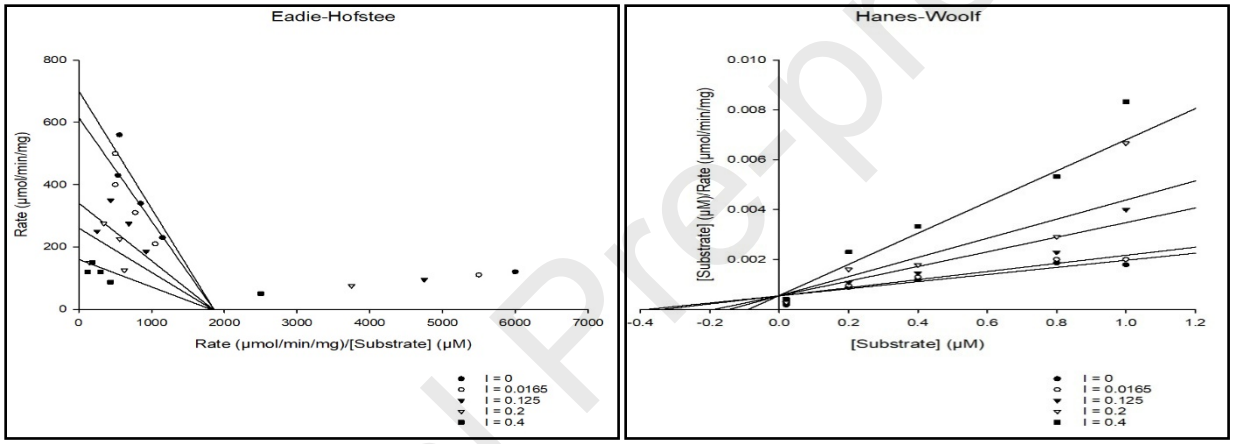

Figure-13:C) Hanes-Woolf plot of compound **33** at different concentration of [S] Vs [S]/Rate in the different concentration of mixed-type inhibitor. **D)** Eadie-Hofstee plot of compound **33** by rate/[S] Vs Rate in the different concentration of mixed-type inhibitor.

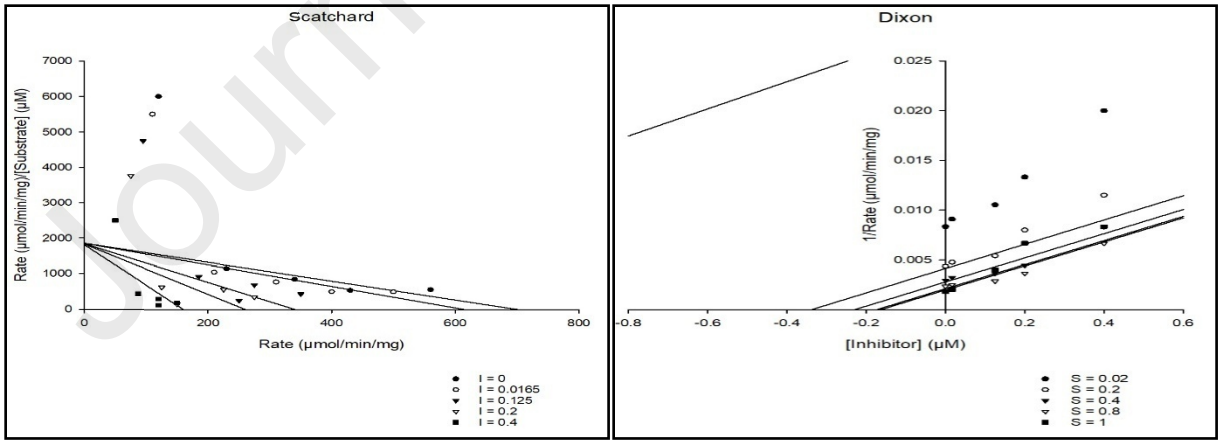

Figure-13:E) Dixon plot of compound **33** at different concentration of mixed inhibitor Vs 1/Rate. **F)** Scatard plot of compound **33** by Rate Vs Rate/[S] in the different concentration of mixed-type inhibitor.

Kinetic characterization of *α*-glucosidase inhibition

Kinetic studies on the most active *α*-glucosidase inhibitors**1**, **14**, **16**, **20**, **21**, **24**, **25**, **27**, **28**, and **33** were carried out to interpret the inhibition mechanism of these compounds. The enzyme inhibition mechanism analyzed by using Sigma-Plot enzyme kinetic software through various parameters as shown in Figure-14 and Table-3. The kinetic studies revealed that the synthetic compounds showed uncompetitive type of inhibition.

Table-3: Kinetic studies of active compounds for *α*-glucosidase inhibition

S. No	Compound. No	Vmax (μM/min)[1]	Km (mM)	AICc	R^2	Type of inhibition
1	**1**	701.4	0.4	201.4	0.985	Uncompetitive type
2	**14**	684.7	0.5	200.4	0.994	Uncompetitive type
3	**16**	680.2	0.5	212.1	0.914	Uncompetitive type
4	**20**	690.5	0.7	213.5	0.984	Uncompetitive type
5	**21**	698.3	0.4	214.2	0.989	Uncompetitive type
6	**24**	701.2	0.5	205.2	0.988	Uncompetitive type
7	**25**	697.1	0.5	200.8	0.901	Uncompetitive type
8	**27**	695.3	0.5	211.7	0.991	Uncompetitive type
9	**28**	684.8	0.5	205.1	0.988	Uncompetitive type
10	**33**	702.7	0.3	199.4	0.994	Uncompetitive type

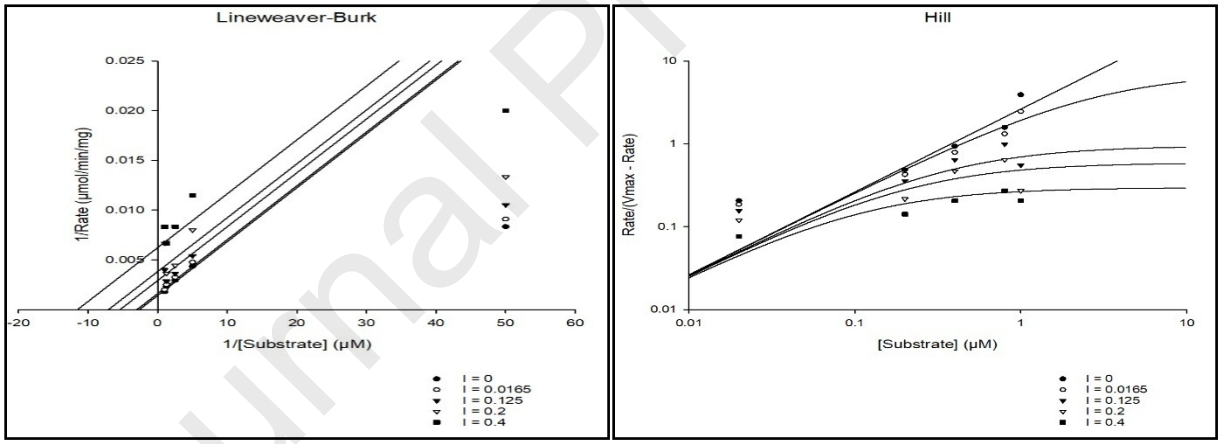

Figure-14:A) Lineweaver-Burk plot of 1/[S] Vs 1/Rate in the different concentration of mixed-type inhibitor. **B)** Hill plot of different concentration of [S] Vs Rate (Vmax-Rate) in the different concentration of mixed-type inhibitor.

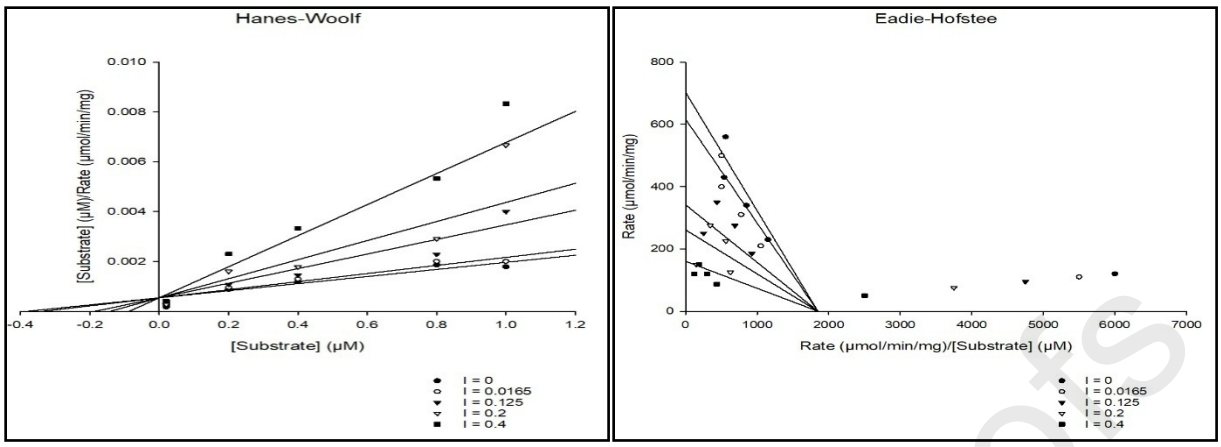

Figure-14:C) Hanes-Woolf plot of compound **33** at different concentration of [S] Vs [S]/Rate in the different concentration of Competitive -type inhibitor. **D)** Eadie-Hofstee plot of compound **33** by rate/[S] Vs Rate in the different concentration of Competitive-type inhibitor.

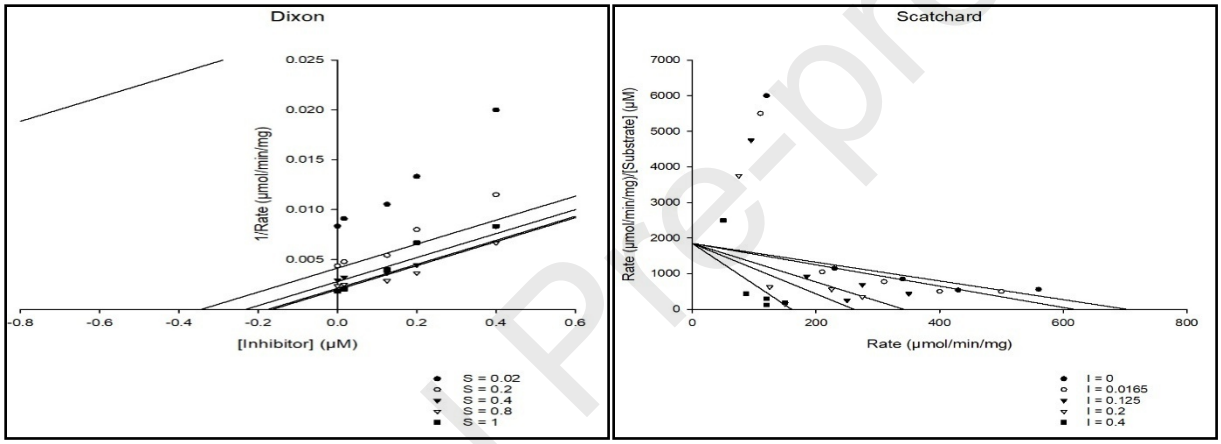

Figure-14:E) Dixon plot of compound **33** at different concentration of competitive inhibitor Vs 1/Rate. **F)** Scatard plot of compound **33** by Rate Vs Rate/[S] in the different concentration of Competitive-type inhibitor.

Molecular Docking (MD) Studies

***α*-Amylase molecular study**

The blind docking (BD) approach was performed to examine the possible binding site of these compounds other than the substrate binding site due to their mixed inhibition nature against the *α*-amylase enzyme. In the mixed type of inhibition, the inhibitor might bind to the protein either the substrate has already linked to the protein or not. The BD study revealed that the derivatives bind to a distinct site other than the substrate binding site with various affinity, as shown in (**Figure-15: A**) (left side). Based on visual inspection, it was perceived that slight conformational changes in the backbone and side-chain of substrate binding residues had been bought, thus gladly supporting the nature of synthetic molecules. In general, the active site of the *α*-amylase enzyme

includes Trp58-59, Tyr151, Leu162, Thr163, Arg195, Asp197-198, 300, Lys200-201, and Glu233 as shown in (**Figure-15: A**) (right side). Afterwards, the BD results revealed that the top active derivatives in the series commonly adopted side-chain donor/acceptor and arene-H interactions including; residue Lys265, Arg319, Asp433, Asn431, and Pro486, respectively. In case of most active derivative **33** in the series adopts side-chain donor and acceptor hydrogen interaction with residue Asn481 and Asp433, while residue Arg319 formed an arene-H bond with the indole pyrrhole ring of the compound (**Figure-15: C**). Based on the visual inspection, we observed that the binding of this compound, bring slight conformational changes in the substrate-binding site and hence might unable the enzyme to produce the product. Derivative **33**, the most active in the series which showed a considerable inhibition as compared to the standard acarbose was presumably an indole ring that exhibits not only favourable interaction with the active site of the enzyme but also showed good docking score comparatively. More interestingly, the 2nd active compound **14** showed a similar binding pattern as was observed for compound **25**, the only difference found was the additional arene-H interaction of D433 adopted with compound **33**. In case of 3rd most active derivatives, compounds **14**, **20**, **21**, and **28** showed similar binding mode with residues Pro485, Asn481, Asp433, and Lys268 (**Figure-15: D-F**), these compounds possess only differences in activity, that might be due to the strength of the bonding interaction as well the distance among the residue and compound. In case of other active derivatives in the series (**1** and **30**) also showed similar interaction with the residues found common Lys268, and with Arg319 compound **16**, and with Pro485 compound **25** as shown in (**Figure-15: G-H**). Overall, the BD and enzyme kinetics study results demonstrate and support the mixed inhibition nature of these derivatives. The binding of these active derivatives to the distinct site other than the substrate-binding site of α-amylase enzyme fetch an active conformational side-chain and backbone changes in the key residues and hence the consequences of changes in the side and backbone chain further reduce the affinity of the substrate against the enzyme. The detail protein-ligand interaction profile listed in (**Table-4**).

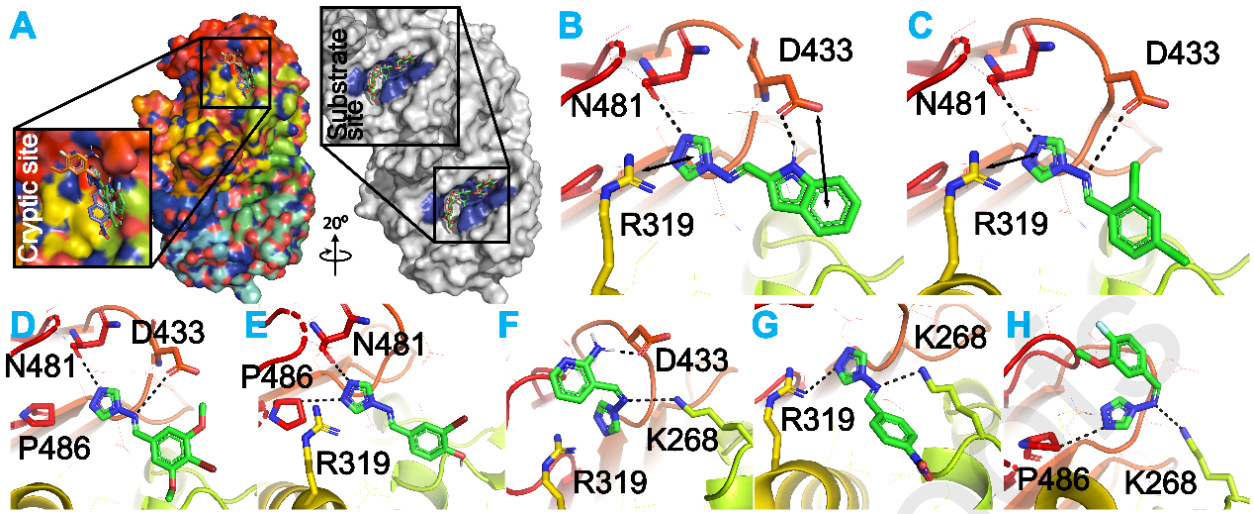

Figure-15: The ligand-protein interaction profile for mixed inhibitors against the *α*-amylase enzyme. **(A)** The surface representation of the alpha-amylase enzyme (PDB ID **3BAJ**), the left side surface representation indicates the distinct binding site (cryptic site) while the right substrate binding site. (**B**) The binding mode of the most potent compound **33**, **(C)** for compound **14**, **(D)** for compound **20**, **(E)** for compound **21**, **(F)** for compound **28, (G)** for compound **16** and **(H)** for compound **25**.

Table-4: Interaction Detail for all derivatives against the *α*-amylase enzyme**.**

S. No.	Interaction details						Docking score
	ligands	receptor		Distance	E cal/mol	residue	
1	5-ring	NH1	π-cation	3.89	-2.7	ARG 319	-4.71
2	O	OD1	H-donor	2.94	-4.4	ASP 433	-4.64
	N	O	H-donor	3.34	-0.6	ASN 431	
	N	CA	H-acceptor	3.58	-0.7	ARG 267	
3	O	OD1	H-donor	2.76	-5.1	ASP 433	-4.99
	N	NZ	H-acceptor	3.56	-1.4	LYS 268	
	5-ring	CD1	π-H	3.85	-0.5	LEU 320	
4	O	O	H-donor	2.86	-1.0	ILE 266	-4.82
	N	CG	H-acceptor	3.48	-0.5	PRO 486	
5	O	OD1	H-donor	2.83	-5.4	ASP 433	-4.00
6	O	CB	H-acceptor	3.54	-0.8	ASN 481	-4.78
	O	ND2	H-acceptor	3.75	-0.5	ASN 481	
7	5-ring	CD1	π-H	3.83	-1.2	LEU 320	-4.67
8	O 18	NZ	H-acceptor	3.35	-0.8	LYS 268	-4.01
	5-ring	CB	π-H	3.62	-0.9	ARG 319	
9	O	CB	H-acceptor	3.54	-0.8	ASN 481	-4.24
10	N 1	CB	H-acceptor	3.55	-0.5	ASN 481	-4.080
	N 2	CG	H-acceptor	3.45	-0.5	PRO 486	
	5-ring	NH1	π-cation	3.89	-3.1	ARG 319	
11	N	CB	H-acceptor	3.66	-0.6	ASN 481	-4.83
	N	NZ	H-acceptor	3.42	-7.9	LYS 268	
	5-ring	NH1	π-cation	3.91	-2.2	ARG 319	
	6-ring	CD1	π-H	3.70	-1.0	LEU 320	
12	N	CG	H-acceptor	3.58	-0.5	PRO 486	-5.03
	5-ring	NH1	π-cation	3.89	-1.9	ARG 319	

13	5-ring	NH1	π-cation	3.88	-2.4	ARG 319	-4.73
14	NH1	OD1	H-donor	3.30	-1.6	ASP 433	-5.92
	N 1	CB	H-acceptor	3.78	-0.6	ASN 481	
	5-ring	NH1	π-cation	3.77	-1.3	ARG 319	
	5-ring	NH1	π-cation	3.87	-1.0	ARG 319	
15	N	O	H-donor	3.34	-0.6	ASN 431	-4.82
	N	CA	H-acceptor	3.58	-0.7	ARG 267	
	O	NH1	H-acceptor	2.91	-4.5	ARG 319	
16	N 1	CB	H-acceptor	3.72	-0.6	ASN 481	-5.32
	5-ring	NH1	π-cation	3.87	-1.2	ARG 319	
17	O 14	O	H-donor	3.37	-0.6	ARG 267	-4.97
	N 3	NH2	H-acceptor	3.59	-1.3	ARG 319	
18	O 7	OD1	H-donor	2.90	-3.3	ASP 433	-4.82
	6-ring	NZ	π-cation	3.91	-0.6	LYS 268	
19	O	OD1	H-donor	2.89	-3.0	ASP 433	-4.81
	5-ring	CB	π-H	3.55	-0.6	ARG 319	
20	N 1	CB	H-acceptor	3.67	-0.5	ASN 481	-5.77
	N 2	CG	H-acceptor	3.53	-0.5	PRO 486	
	NH1	OD1	H-donor	3.50	-2.6	ASP 433	
21	N	CG	H-acceptor	3.48	-0.5	PRO 486	-5.59
	N	CB	H-acceptor	3.56	-0.5	ASN 481	
22	O 14	OD1	H-donor	2.82	-5.5	ASP 433	-4.030
	O 2	CG	H-acceptor	3.59	-0.6	PRO 486	
	O 6	NZ	H-acceptor	3.26	-8.4	LYS 268	
23	N	O	H-donor	3.34	-0.6	ASN 431	-4.77
	N	CA	H-acceptor	3.58	-0.7	ARG 267	
	O	NH1	H-acceptor	2.91	-4.5	ARG 319	
24	N 2	CG	H-acceptor	3.55	-0.5	PRO 486	-4.71
	N 3	CB	H-acceptor	3.64	-0.6	ASN 481	
	5-ring	NH1	π-cation	3.88	-2.0	ARG 319	
25	N	NZ	H-acceptor	3.59	-3.5	LYS 268	-5.49
	5-ring	NH1	π-cation	3.67	-2.4	ARG 319	
26	N	CB	H-accepter	3.41	-0.5	ASN 481	-4.64
27	O 7	OD1	H-donor	3.32	-0.7	ASN 431	-4.76
	O 10	ND2	H-acceptor	2.99	-4.0	ASN 481	
28	N 14	OD1	H-donor	2.95	-3.0	ASP 433	-5.51
	N 6	NZ	H-acceptor	3.87	-1.7	LYS 268	
29	N 1	CG	H-acceptor	3.49	-0.5	PRO 486	-4.44
	N 2	CB	H-acceptor	3.60	-0.5	ASN 481	
	5-ring	NH1	π-cation	3.86	-2.9	ARG 319	
30	N 1	CB	H-acceptor	3.57	-0.7	ASN 481	-4.49
	N 6	NZ	H-acceptor	3.42	-7.3	LYS 268	
	5-ring	NH1	π-cation	3.91	-2.4	ARG 319	
	6-ring	CD1	π-H	3.72	-1.0	LEU 320	
31	5-ring	NH1	π-cation	3.95	-4.7	ARG 319	-4.83
	5-ring	NH2	π-cation	3.73	-0.5	ARG 319	
32	6-ring	CD	π-H	3.70	-0.6	ARG 319	-4.97
33	N 3	CB	H-acceptor	3.55	-0.6	ASN 481	-6.53
	5-ring	NH1	π-cation	3.92	-2.2	ARG 319	
	5-ring	NH2	H-acceptor	3.86	-0.5	ASP 433	
	NH1	OE1	π-cation	3.42	-2.3	ASP 433	

α-Glucosidase molecular study

The blind docking (BD) approach was performed to explore the possible binding mode of the synthetic inhibitors in the binding site other than the substrate binding site due to the uncompetitive inhibition type of the synthesis derivatives against the α-glucosidase enzyme. The BD results revealed that all the derivatives bind to a site; cryptic site, other than substrate-binding site with various affinity due to the uncompetitive nature as shown in (**Figure-16A**) and (**Table-5**). The deep insight protein-ligand interaction (PLI) analysis revealed that mostly the active inhibitors which showed high potency against the corresponding enzyme adopt various interaction with acidic, basic and polar residues, amino acid includes Asp68, Asp214, Glu276, Asp408, and Glu304, basic include Arg439 and His111 which is polar and with the benzyl side chain of the non-polar, essential amino acid Phe157, respectively. More interestingly, the indole pyrrhole ring of all the inhibitors showed similar interaction with the acidic residue Asp214 this might play a crucial role in enhancing the catalytic activity of the enzyme. In case of the most potent inhibitor compound, **33** in the series showed favourable binding mode in the cryptic site of against α-glucosidase enzyme and adopted side-chain donor interaction only with acidic residues including Asp214, Asp68, Glu276 and Glu304 (**Figure-16B**). Moreover, the other active derivative in the series compound **25** showed similar binding mode with residues acidic side chain residues Asp68, Asp214, and hydrophobic side chain residue Phe157 (**Figure-16C**). The only differences found was the additional interaction adopted by compound **25** instead of Asp68 with the aliphatic amino acid Lys155. In case of other active compounds **27** and **24** found in adopting side-chain acceptor and donor interaction with the acidic residue Asp214 and with polar side chain His111 (**Figure-16D-F**). Overall, the high potency of these compounds might be based on the favourable interaction adopted by the indole pyrrhole ring of the compounds with the acidic residue Asp214 and with another residue. Additionally, the BD study and enzyme kinetics study results demonstrate and support the uncompetitive nature of these compounds.

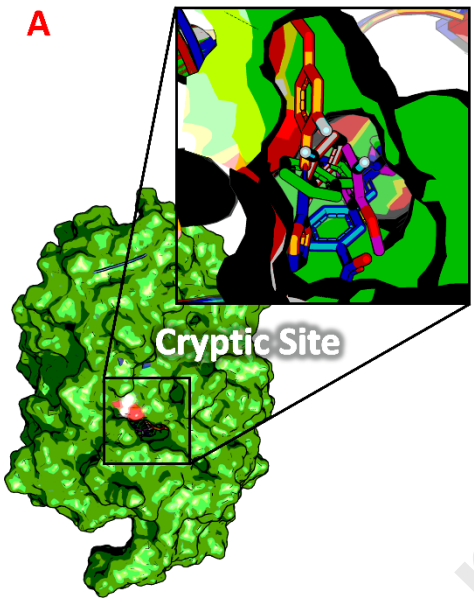

Figure-16: The ligand-protein interaction (LPI) profile for uncompetative inhibitors against α-glucosidase enzyme. **(A)** The surface representation of the cryptic site aprt from substrate binding site due to the uncompetative type of inhibiton of the compounds

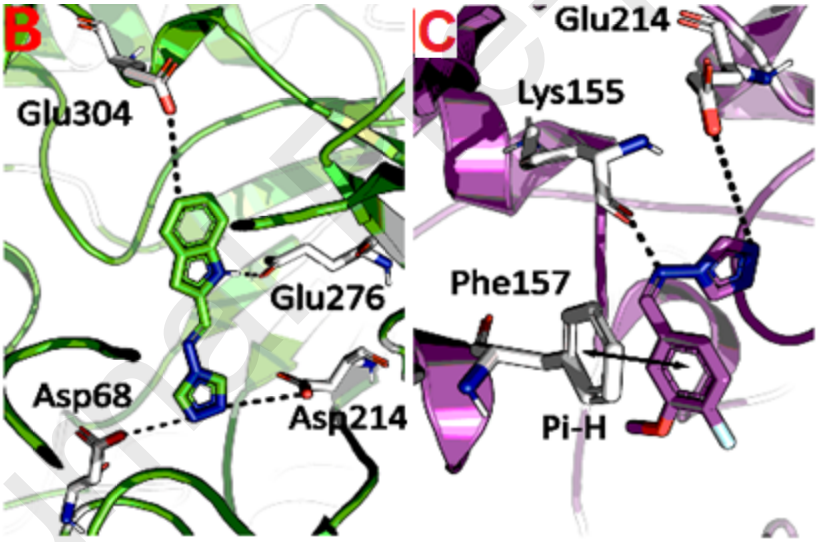

Figure-16: (B) The binding mode of the most potent compound **33 (C)** for compound **25**

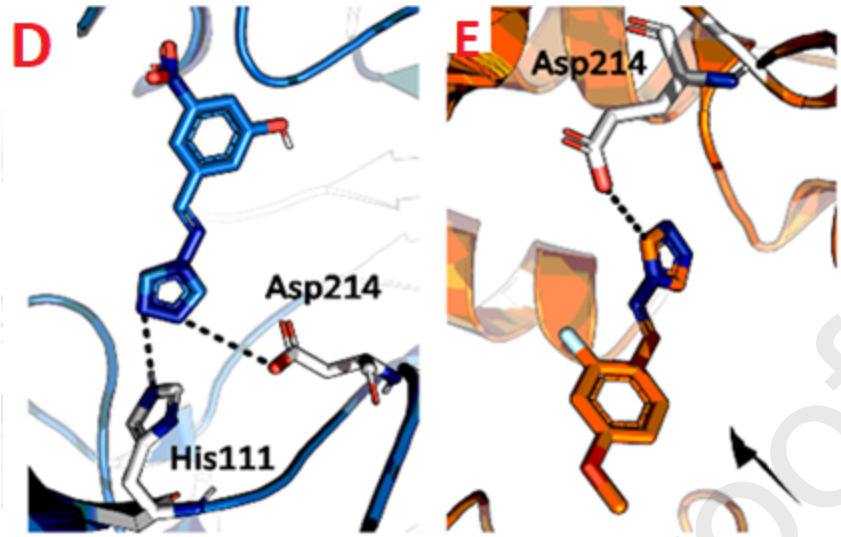

Figure-16: The binding mode of the most potent compound **(D)** for compound **27 (E)** for compound **24**

Table-5: Interaction Detail for all compounds against *α*-glucosidase enzyme**.**

S. No	Interaction Report						Docking score
	Ligand	Receptor	Interaction	Distance	E (kcal/mol)	Residue	
1	O 14	OD1	H-donor	3.10	-1.3	ASN 412	-5.33
2	O 14 O 14	OD1 OD2	H-donor H-donor	2.84 3.18	-5.0 -0.5	ASP 214 ASP 214	-5.31
3	O 15	OE1	H-donor	2.84	-3.3	GLU 276	-5.04
4	O 15	N	H-acceptor	3.10	-1.1	TRP 136	-4.93
5	O 16	OG1	H-donor	2.97	-1.4	THR 307	-5.10
6	C 10	5-RING	H-π	3.92	-0.5	HIS 245	-5.44
7	C 1	OE1	H-donor	3.48	-0.6	GLU 276	-5.24
8	C 7 C 13	5-RING 5-RING	H-π H-π	4.31 4.08	-0.6 -1.7	HIS 245 HIS 245	-5.93
9	N 3	NE2	H-acceptor	3.01	-1.2	HIS 111	-6.32
10	N 1	NE2	H-acceptor	3.00	-1.0	HIS 111	-6.34
11	N 3	NE2	H-acceptor	3.05	-1.2	HIS 111	-5.58
12	N 1	NE2	H-acceptor	2.92	-1.2	HIS 111	-5.81
13	N 3	NE2	H-donor	3,12	-1.0	HIS 111	-4.93
14	N 1	NE2	H-acceptor	3.02	-1.2	HIS 111	-5.54
15	O 15	NE2	H-acceptor	3.05	-1.3	HIS 111	-5.72
16	N 1	NE2	H-acceptor	3.09	-1.1	HIS111	-5.52
17	C 1	OD1	H-donor	3.14	-0.8	ASP 214	-5.61
18	O 7	OE1	H-donor	2.77	-4.4	GLU 276	-5.41
19	N 3	NE2	H-acceptor	3.07	-1.1	HIS 111	-5.79
20	5-RING	CD2	π-H	3.79	-0.5	LEU 218	-5.65
21	N 3	NE2	H-acceptor	3.03	-1.1	HIS 111	-5.48
22	6-RING	CA	π-H	4.02	-0.8	PHE 157	-5.64
23	BR 14	OD1	H-donor	3.44	-4.6	ASP 214	-5.48
24	C 4	OE2	H-donor	3.61	-0.6	GLU 214	-5.4

25	N1 6-RING N 4	OD1 CA NZ	H-donor π-H H-acceptor	3.2 3.08 3.5	-4.3 -1.3 -2.9	ASP 214 PHE 157 LYS155	-6.15
26	O 16	NE2	H-acceptor	3.20	-0.7	HIS 111	-5.92
27	C 17 N 13	OD1 NE2	H-donor H-acceptor	3.38 3.09	-0.5 -1.3	ASP 214 HIS 111	-5.54
28	6-RING 5-RING	CA CB	π-H π-H	4.02 4.24	-1.0 -0.8	PHE 157 ARG 312	-4.73
29	N 1	N	H-acceptor	3.56	-1.4	GLY 217	-6.16
30	N 1	NE2	H-acceptor	3.08	-1.0	HIS 111	-6.83
31	C 4	OD2	H-donor	3.50	-0.9	ASP 408	-5.77
32	6-RING	CD2	π-H	4.07	-0.7	HIS 279	-6.20
33	C 1 N 9 C2 N3	OD1 OE1 OD1 OE1	H-donor H-donor H-donor H-donor	3.20 3.04 3.10 3.14	-0.6 -4.8 -0.5 -4.5	ASP 214 GLU 276 ASP 214 GLU 276	-7.29

Conclusion:

Novel derivatives of 4-amino-1,2,4-triazole (**1-33**) have been synthesized by reacting 4-amino-1,2,4-triazole with different substituted benzaldehydes in ethanol under reflux. The synthetic molecules were characterized *via* ^{1}H-NMR and EI-MS spectroscopic techniques and evaluated for their α-amylase and α-glucosidase inhibition. These compounds demonstrated good inhibitory activity against both enzymes and found to be dual and potential inhibitors of α-amylase and α-glucosidase enzymes. Among thirty three derivatives, ten compounds **1**, **14**, **16**, **20**, **21**, **24**, **25**, **27**, **28**, and **33** showed superior activity in the range of IC_{50} value of 2.01-2.09 against α-amylase and 2.09-2.62 μM against α-glucosidase enzymes, respectively, however, other compounds were moderately active. Compound **33** (IC_{50} = 2.01 ± 0.03 μM) (IC_{50} = 2.09 ± 0.08 μM) with an indole ring as aryl part was found to be the most potential inhibitor of both enzymes might be due to the better interactions of indole ring with the active site of enzyme. Kinetic studies revealed that the synthetic analogs have exhibited mixed type of inhibition against α-amylase and uncompetitive type of inhibition against α-glucosidase enzymes. The *in silico* studies have supported and identified the binding interactions of these synthetic molecules with the enzyme. In conclusion, these compounds may serve as lead molecules for further drug development studies that may help to control hyperglycemia thus in future they may serve as drug candidates for the treatment of diabetes.

Materials and methods

Thin layer chromatography was carried out on pre-coated silica gel, GF-254 (Merck, Germany). Spots were visualized under ultraviolet light at 254, 366 nm or iodine vapors. EI-MS spectra were recorded on MAT 312 and MAT 113D mass spectrometers. The ^{1}H-NMR were recorded on a Bruker AM spectrometers, operating at 300 and 400 MHz. The chemical shift values are presented in ppm (δ), relative to tetramethylsilane (TMS) as an internal standard and the coupling constant (J) are in Hz. Melting points of the compounds were determined on a Stuart® SMP10 melting point apparatus and are uncorrected.

Kinetic Study Assay

***α*-Amylase inhibition assay**

To determine the mechanism of enzyme inhibition, the kinetic studies were performed by using varying concentration of α-amylase inhibitors (0.0625, 0.125, 0.3 and 0.4 mM) with varying concentrations of inhibitor substrate (*p*-nitrophenyl-R-D-maltoside (NPM)) such as 0.1, 0.2, 0.4, 0.8, and 1.0 mM. The enzyme was dissolved in de-ionized water to produce the concentration 0.2 mg/mL for each well. PIPES buffer was adjusted at the pH of 7.0, the reaction mixture was incubated for the period of 30 minutes at 25 $^{\circ}$C. The absorbance was measured using ELISA reader by keeping the 96-well plate (BioTek XL-800, USA). The kinetic parameters Vmax, Km, AICc and R^2 values of all the α-amylase inhibitor activities were determined by graph fitting analysis using Sigma-Plot enzyme kinetic software 14.0 version [29-30]

***α*-Glucosidase inhibition assay**

To determine the mechanism of α-glucosidase enzyme inhibition, the kinetic studies were performed by using varying concentration of α-glucosidase inhibitors (0.0625, 0.125, 0.3 and 0.4 mM) with varying concentrations of inhibitor substrate (*p*-nitrophenyl R-D-maltoside (NPM)) such as 0.1, 0.2, 0.4, 0.8 and 1.0 mM. The enzyme was dissolved in de-ionized water to produce the concentration 0.2 mg/mL for each well. PIPES buffer was used at the pH of 7.0. The reaction mixture was incubated for the period of 30 minutes at 25 $^{\circ}$C for 1-minute interval. The absorbance was measured using ELISA reader by keeping the 96-well plate (BioTek XL-800, USA). The kinetic parameters Vmax, Km, AICc and R^2 values of all the α-glucosidase inhibitors were determined by graph fitting analysis using Sigma-Plot enzyme kinetic software 14.0 version [27].

Enzyme Inhibition Assays

α-Amylase Inhibition assay

The *α*-amylase inhibitory activity was determined by an assay modified from Kwon, Apostolidis and Shetty. A volume of 500 *μ*L of *α*-amylase solution (0.5 mg/mL) in 0.2 mM phosphate buffer (pH 6.9) and 500 *μ*L of test sample (100, 200, 400, 800, 1000 *μ*g/mL) were incubated for 10 min at 25 ˚C. After pre-incubation, 1% starch solution (500 *μ*L) in 0.02 M sodium phosphate buffer (pH 6.9) was added to each tube and incubated at 25 ˚C for 10 min. 1 mL of dinitrosalicylic acid color reagent was then added to the reaction mixture and the tubes were incubated in boiling water for 5 min, and finally cooled to room temperature. The solutions were diluted by adding 10 mL distilled water and the absorbance was measured at 540 nm [24]. The percentage inhibition was calculated as illustrated,

$$\% \text{ Inhibition} = (\text{Absorbance}_{\text{Control}} - \text{Absorbance}_{\text{Sample}})/\text{Absorbance}_{\text{Control}} \times 100$$

α-Glucosidase Inhibition assay

Rat intestinal acetone powder in typical saline (100:1; w/v) was sonicated appropriately and the supernatant was used as a source of basic intestinal *α*-glucosidase after centrifugation. In short,10 mL of test samples of 5 mg/mL in DMSO solution were reconstituted in 100 mL of 100 mM-phosphate buffer at pH 6.8 in 96-well micro-plate and incubated with 50 mL of basic intestinal *α*-glucosidase for five min before 50 mL substrate (5 mM, *p*-nitrophenyl-*α*-D-glucopyranoside prepared in same buffer) was added *p*-nitro-phenol released was measured at 405 nm spectrophotometrically (Spectra Max plus384, Molecular Devices Corporation, Sunnyvale, CA, USA) 5 min after incubation with the substrate. Individual blanks for test samples were prepared to accurate background absorbance where the substrate was changed with 50 mL of buffer. Control sample contained 10 mL DMSO beside test samples. Percentage of enzyme inhibition was measured as (1B/A) 100 where [A] represents absorbance of control exclusive of test samples, and [B] corresponding to absorbance in presence of test samples [15].

Molecular Docking Protocol

***α*-Amylase inhibition**

By using various kinetics plots, such as Lineweaver-Burk, Hill, Hanes-Woolf, Eadie-Hofstee, Dixon and Scatchard models, the kinetic parameters Vmax, Km, AICc and R^2 values were calculated (**Table-2**). Based on curve fitting model and low AICc value, the kinetic studies results revealed that all the selected compounds following mixed type inhibitors mechanism. However, due to the mixed type of inhibition nature of the synthesised derivatives, blind docking (BD) was performed of the derivatives against *α*-amylase enzyme using Molecular operating environment (MOE)® software package [31]. Before proceeding the BL approach, the 3D structural coordinates of alpha-amylase (PDB code 3BAJ) was retrieved from Protein Data Bank (www.rcsb.org). Then, briefly followed the structure preparation step implemented in MOE. The 3D structures for all the derivatives were built by using the Molecular Builder Module in MOE. Next, the whole protein was considered as a binding site to dock the mixed type inhibitors against *α*-amylase enzyme blindly. Subsequently, all the derivatives were then docked into; using the whole protein as a binding site and a total of 50 different conformations for each compound allowed to generate. The ligands were set to flexible during docking so that to obtain minimal energy complex. Later on, the docked complexes were ranked based on the docking scores (S). Finally, the predicted ligand-protein complexes were analysed for molecular interactions using **PyMol** v 1.7.

***α*-Glucosidase inhibition**

Blind docking (BD) approach was performed using MOE-dock module implemented in Molecular Operating Environment (MOE) software package [28] of all the uncompetitive type synthesized derivatives against α-glucosidase enzyme. Due to the unavailability of crystallographic structure of the corresponding enzyme, we used the homology modelling structural coordinates as described by Carreiro et al [32] for α-glucosidase enzyme. Next, the whole protein was considered as a binding site for the purpose of BD based on two reason; due to the cryptic binding site and uncompetitive type of inhibition as well. Briefly, the homology model was subjected for 3D protonation and energy minimization up to 0.05 Gradient using MMFF94s force field implemented in MOE software. The 3D structures were built by using Molecular Builder Module in MOE. All the inhibitors were then docked using the whole protein as a binding site and total 50 different conformations for each inhibitor allowed to generate. The ligands be flexible during docking, so

that to obtain minimal energy complex. Later, the docked complexes were ranked based on the docking scores (S). Finally, the predicted ligand-protein complexes were analyzed for molecular interactions using **PyMol** v 1.7.

Spectral data of Synthetic compounds (1-33)

4-(((4*H*-1,2,4-Triazol-4-yl)imino)methyl)phenol (1)

Off-white powder, Yield: 0.27 g (78%); ^{1}H-NMR: (400 MHz, DMSO-d_6) δ 10.33 (br.s, 1H, OH-4'), 9.10 (s, 2H, H-3, H-5), 8.92 (s, 1H, -N=CH), 7.71 (d, $J_{2',6'}$ = 8.8 Hz, 2H, H-6', H-2'), 6.92 (d, $J_{3',5'}$ = 8.8 Hz, 2H, H-3', H-5'). EI-MS: *m/z* (rel. abund. %) 188 (M^+, 100), 189 (M^++1, 13), 106 (25), 105 (14).

4*H*-1,2,4-Triazol-4-ylimino)methyl)benzene-1,2-diol (2)

White powder, Yield: 0.2 g (71%), M.p: 266-268 ˚C; ^{1}H-NMR: (400 MHz, DMSO-d_6) δ 9.67 (br.s, 2H, OH-2', H-6'), 9.14 (s, 2H, H-3, H-5), 9.13 (s, 1H, N=CH), 7.23 (dd, $J_{3',4'}$ = 8.0 Hz, $J_{3',5'}$ = 1.2 Hz, 1H, H-3'), 6.97 (dd, $J_{5',4'}$ = 7.6 Hz, $J_{5',3'}$ = 1.2 Hz, 1H, H-5'), 6.78 (t, $J_{4',3',5'}$ = 8.0 Hz, 1H, H-4'); EI-MS: *m/z* (rel. abund. %): 204 (M^+, 50), 135 (100), 107 (33), 70 (40), 69 (42), 52 (20), 42 (18).

4-((4*H*-1,2,4-Triazol-4-ylimino)methyl)benzene-1,3-diol (3)

Green powder, Yield: 0.2 g (84%), M.p: 288-289 ˚C; ^{1}H-NMR: (400 MHz, DMSO-d_6) δ 10.33 (br.s, 2-OH, OH-3', OH-4'), 9.05 (s, 2H, H-3, H-5), 8.95 (s, 1H, -N=CH), 7.60 (d, $J_{6',5'}$ = 9.2 Hz, 1H, H-6'), 6.39 (overlapping multiplet, 2H, H-3', H-5'). EI-MS: *m/z* (rel. abund. %) 204 (M^+, 100), 148 (4), 227 (90), 135 (94), 201 (76), 121 (8), 100 (4), 108 (23), 94 (20), 64 (41), 66 (11), 42 (12).

2-((4*H*-1,2,4-triazol-4-ylimino)methyl)benzene-1,4-diol (4)

Light green powder, Yield: 0.2 g (79%), M.p: 286-287 ˚C; ^{1}H-NMR: (400 MHz, DMSO-d_6) δ 9.74 (br.s, 1H, OH-2'), 9.12 (s, 2H, H-3, H-5), 9.11 (br.s, 1H, OH-3'), 9.04 (s, 1H, -N=CH), 7.17 (d, $J_{6',3'}$ = 2.8 Hz, 1H, H-6′), 6.87 (m, 2H, H-3', H-4'); EI-MS: *m/z* (rel. abund. %): 204 (M^+, 7), 135 (100), 107 (77), 79 (32), 69 (67), 52 (66), 42 (42).

4-(((4H-1,2,4-triazol-4-yl)imino)methyl)benzene-1,2,3-triol (5)

White powder, Yield: 0.22 g (88%), M.p.: 285-287 ˚C; ^{1}H-NMR: (400 MHz, DMSO-d_6) δ 9.95 (s, 1H, OH-2'), 9.73 (s, 1H, OH-4'), 9.07 (s, 2H, H-3, H-5), 8.97 (s, 1H, -N=CH), 8.65 (br.s, 1H, OH-3'), 7.09 (d, $J_{6',5'}$ = 8.8 Hz, 1H, H-6'), 6.46 (d, $J_{5',6'}$ = 8.8 Hz, 1H, H-5'). EI-MS: *m/z* (rel. abund. %) 220 (M^+, 100), 151 (62), 70 (62), 67 (20).

1-(2,4-Dimethoxyphenyl)-*N*-(4*H*-1,2,4-triazol-4-yl)methanimine (6)

Off-white powder, Yield: 0.12 g (68 %), M.p.: 239- 240 ˚C; ^{1}H-NMR: (400 MHz, DMSO-d_6) δ 9.08 (s, 2H, H-3, H-5), 8.96 (s, 1H, -N=CH), 7.42 (d, $J_{3',5'}$ = 2.0 Hz, H, H-3'), 7.39 (dd, $J_{5',3'}$ = 1.6 Hz, $J_{5',6'}$ = 8.4 Hz, 1H, H-5'), 7.14 (d, $J_{6',5'}$ = 8.4 Hz, 1H, H-6'), 3.84 (s, 3H, CH_3-4') 3.82 (s, 3H, CH_3, H-1'). EI-MS: *m/z* (rel. abund. %) 232 (M^+, 100), 233 (M^++1, 43), 163 (11), 73 (11).

(2,6-Dimethoxyphenyl)-*N*-(4*H*-1,2,4-triazol-4-yl)methanimine (7)

White powder, Yield: 0.22 g (94%), M.p.: 147-149 ˚C; ^{1}H-NMR: (400 MHz, DMSO-d_6) δ 9.38 (s, 2H, H-3, H-5), 9.04 (s, 1H, -N=CH), 7.54 (t, $J_{4',3'/5',4'}$ = 8.4 Hz, 1H, H-4'), 6.81 (d, $J_{3',5'}$ = 8.4 Hz, 2H, H-3', H-5'), 3.84 (s, 6H, OCH_3-2', OCH_3-6'). EI-MS: *m/z* (rel. abund. %) 232 (M^+, 62), 164 (25), 149 (100), 121 (42), 107 (22), 91 (64), 77 (26).

***N*-(3,4,5-Trimethoxybenzylidene)-4*H*-1,2,4-triazol-4-amine (8)**

White powder, Yield: 0.3 g (92%); ^{1}H-NMR: (400 MHz, DMSO-d_6) δ 9.22 (s, 2H, H-3, H-5), 9.02 (s, 1H, -N=CH), 7.16 (s, 2H, H-2', H-6'), 3.84 (s, 6H, 3'-OCH_3, 5'-OCH_3), 3.74 (s, 3H, H-4'-OCH_3); EI-MS: *m/z* (rel. abund. %): 262 (M^+, 26), 248 (12), 247 (90), 150 (22), 64 (10).

***N*-(4-Ethoxy-3-methoxybenzylidene)-4*H*-1,2,4-triazol-4-amine (9)**

Light-yellow powder, Yield: 0.16 g (73%), M.p: 200-201 ˚C; ^{1}H-NMR: (400 MHz, DMSO-d_6) δ 9.37 (s, 2H, H-3, H-5), 8.99 (s, 1H, N=CH), 7.43 (s, 1H, H-2'), 7.39 (d, $J_{5',6'}$ = 8.4 Hz, 2H, H-5', H-6′), 7.14 (d, $J_{6',5'}$ = 8.4 Hz, 1H, H-6'), 4.55 (q, 2H, OCH_2-4'), 3.82 (s, 3H, H-OCH_3), 1.37 (t, $J_{CH3-CH2}$ = 6.8 Hz, 3H, CH_3-4'); EI-MS: *m/z* (rel. abund. %) 246 (M^+, 100), 218 (35), 134 (23), 149 (29), 122 (55), 70 (14).

***N*-(3-Ethoxy-4-methoxybenzylidene)-4*H*-1,2,4-triazol-3-amine (10)**

White powder, Yield: 0.18 g (75%), M.p.: 198-200 ˚C; ^{1}H-NMR: (400 MHz, DMSO-d_6) δ 9.16 (s, 2H, H-3, H-5), 8.97 (s, 1H-N=CH), 7.42 (d, $J_{2',6'}$ = 1.6 Hz, 1H, H-2'), 7.37 (dd, $J_{6',2'}$ = 1.6 Hz, $J_{6',5'}$ = 6.4 Hz, 1H, H-6'), 7.13 (d, $J_{5',6'}$ = 8.4 Hz, 1H, H-5'), 4.13 (t, $J_{CH2,\ CH3}$ = 8.0 Hz, 2H, -OCH_2), 3.82 (s, 3H, OCH_3), 1.37 (t, $J_{CH3,\ CH2}$ = 8.0 Hz, 3H, CH_3-4'); EI-MS: *m/z* (rel. abund. %): 246 (M^+, 100), 218 (25), 149 (11), 136 (18), 122 (41), 70 (10).

(2,4-Dimethylphenyl)-*N*-(4*H*-1,2,4-triazol-4-yl)methanimine (11)

White powder, Yield: 0.15 g (62%), M.p.: 173-175 ˚C; ^{1}H-NMR: (400 MHz, DMSO-d_6) δ 9.15 (s, 2H, H-3, H-5), 9.11 (s, 1H, N=CH), 7.81 (d, $J_{3',5'}$ = 8.4 Hz, 1H, H-3'), 7.16 (m, 2H, H-5', H-6'), 2.51 (s, 3H, H-2'), 2.32 (s, 3H, H-4'). EI-MS: *m/z* (rel. abund. %) 200 (M^+, 70), 184 (16), 144 (100), 169 (22), 118 (100), 130 (64), 117 (90), 103 (32), 91 (30).

***N*-(4-*tert*-butylbenzylidene)-4*H*-1,2,4-triazol-4-amine (12)**

White powder, Yield: 0.15 g (63%), M.p.: 162-163 ˚C; ^{1}H-NMR: (400 MHz, DMSO-d_6) δ 9.12 (s, 2H, H-3, H-5), 9.05 (s, 1H, -N=CH), 7.79 (d, $J_{2',6'}$ = 8.4 Hz, 2H, H-2', H-6'), 7.59 (d, $J_{3',5'}$ = 8.4 Hz, 2H, H-3', H-5'), 1.30 (s, 6H, CH_3-4'), 1.22 (s, 3H, CH_3-4'). EI-MS: *m/z* (rel. abund. %) 228 (M^+, 41), 213 (100), 144 (31), 115 (16), 91 (14), 70 (48).

(4-Chlorophenyl)-*N*-(4*H*-1,2,4-triazol-4-yl)methanimine (13)

White powder, Yield: 0.10 g (72%), M.p.: 193-195 ˚C; ^{1}H-NMR: (400 MHz, DMSO-d_6) δ 9.12 (s, 2H, H-3, H-5), 9.09 (s, 1H, -N=CH), 7.87 (d, $J_{2',6'} = J_{6',2'}$ = 8.4 Hz, 2H, H-2', H-6'), 7.64 (d, $J_{3',5'} = J_{5',3'}$ = 8.4 Hz, 2H, H-3', H-5'). EI-MS: *m/z* (rel. abund. %) 206 (M^+, 100), 208 (M^++2, 43) 138 (10), 137 (22), 124 (36), 89 (47).

***N*-(2,4-Dichlorobenzylidene)-4*H*-1,2,4-triazol-4-amine (14)**

Light yellow powder, Yield: 0.17 g (69%), M.p: 167-168 ˚C; ^{1}H-NMR: (400 MHz, DMSO-d_6) δ 9.23 (s, 2H, H-3, H-5), 9.17 (s, 1H, -N=CH), 8.06 (d, $J_{6',5'}$ = 8.4 Hz, 1H, H-6'), 7.85 (d, $J_{3',5'}$ = 1.6 Hz, 1H, H-3'), 7.62 (dd, $J_{5',6'}$ = 6.8 Hz, $J_{3',5'}$ = 1.6 Hz, 1H, H-5'); EI-MS: *m/z* (rel. abund. %) 240 (M^+, 62), 242 (M^++2, 32), 244 (M^++4, 5), 207 (60), 205 (100), 158 (47), 123 (93), 61 (17).

***N*-(3-Nitrobenzylidene)-4*H*-1,2,4-triazol-4-amine (15)**

White powder, Yield: 0.20 g (99%), M.p: 248-249 ˚C; ^{1}H-NMR: (400 MHz, DMSO-d_6) δ 9.27 (s, 1H, N=CH), 9.18 (s, 2H, H-3, H-5), 8.62 (s, 1H, H-2'), 8.43 (dd, $J_{6',5'}$ = 8.0 Hz, $J_{6',2'}$ = 1.6 Hz, 1H, H-6'), 8.26 (d, $J_{4',5'}$ = 8.0 Hz, 1H, H-4'), 7.88 (t, $J_{5',6',4'}$ = 8.0 Hz, H-5'); EI-MS: *m/z* (rel. abund. %): 217 (M^+, 100), 170 (29), 116 (20), 103 (14), 89 (87), 76 (15), 63 (20).

***N*-(4-Nitrobenzylidene)-4*H*-1,2,4-triazol-4-amine (16)**

Yellow powder, Yield: 0.25g (91%), M.p: 267-269˚C; ^{1}H-NMR: (400 MHz, DMSO-d_6) δ 9.24 (s, 1H, -N=CH), 9.19 (s, 2H, H-3, H-5), 8.40 (d, $J_{3',5'} = J_{5',3'}$ = 8.8 Hz, 2H, H-3', H-5'), 8.10 (d, $J_{2',6'} = J_{6',2'}$ = 8.8 Hz, 2H, H-2', H-6'); EI-MS: *m/z* (rel. abund. %) 217 (M^+, 158), 162 (14), 116 (30), 89 (100).

4-((4*H*-1,2,4-Triazol-4-ylimino)methyl)-2,5-di-*tert*-butylphenol (17)

White powder, Yield: 0.19 g (68%), M.p: 209-210 ˚C; ^{1}H-NMR: (400 MHz, DMSO-d_6) δ 9.06 (s, 2H, H-3, H-5), 8.95 (s, 1H, N=CH), 7.77 (s, 1H, OH-4'), 7.67 (overlapping multiplet, 2H, H-3', H-6'), 1.41 (s, 18H, (CH_3)-2', (CH_3)-5'); EI-MS: *m/z* (rel. abund. %): 300 (M^+, 34), 285 (68), 216 (100), 188 (28), 70 (46).

5-((4*H*-1,2,4-Triazol-4-ylimino)methyl)-2-methoxyphenol (18)

Light yellow powder, Yield: 0.21 g (96%), M.p: 230- 231 ˚C; ^{1}H-NMR: (400 MHz, DMSO-d_6) δ 9.20 (s, 2H, H-3, H-5), 8.90 (s 1H, N=CH), 7.32 (d, $J_{2',6'}$ = 2.5 Hz, 1H, H-2'), 7.26 (dd, $J_{6',5'}$ = 8.4 Hz, $J_{6',2'}$ = 2.5 Hz, 1H, H-6'), 7.09 (d, $J_{5',6'}$ = 8.4 Hz, 1H, H-5'); EI-MS: *m/z* (rel. abund. %) 218 (M^+, 100), 149 (21), 122 (96), 93 (10), 70 (74), 65 (20), 51(59).

4-(-(4*H*-1,2,4-Triazol-4-ylimino)methyl)-2,6-dimethoxyphenol (19)

Light yellow powder, Yield: 0.25 g (87%), M.p.: 275-276 ˚C; ^{1}H-NMR: (400 MHz, DMSO-d_6) δ 9.18 (s, 2H, H-3, H-5), 8.93 (s, 1H, -N=CH), 7.13 (s, 2H, H-2', H-6'), 3.83 (s, 3H, H-3'-OCH_3), 3.71 (s, 3H, OCH_3-5'); EI-MS: *m/z* (rel. abund. %) 248 (M^+, 100), 179 (14), 164 (7), 152 (37), 123 (13).

***N*-(4-Bromo-3,5-dimethoxybenzylidene)-4*H*-1,2,4-triazol-4-amine (20)**

White powder, Yield: 0.31 g (99%), M.p: 239-240 ˚C; ^{1}H-NMR: (400 MHz, DMSO-d_6) δ 9.15 (s, 2H, H-3, H-5'), 9.08 (s, 1H, N=CH), 7.17 (s, 2H, H-2', H-6'), 3.91 (s, 6H, OCH_3-3', OCH_3-5'); EI-MS: *m/z* (rel. abund. %) 311 (M^+, 50), 313 (M^++2, 49), 310 (100), 280 (4), 243 (30), 149 (48), 69 (36).

5-((4*H*-1,2,4-Triazol-4-ylimino)methyl)-2-bromophenol (21)

White powder, Yield: 0.2 g (72%), M.p: 253- 254 ˚C; ^{1}H-NMR: (400MHz, DMSO-d_6) δ 11.20 (br.s, 1H, OH-4'), 9.05 (s, 2H, H-3, H-5), 8.92 (s, 1H-N=CH), 7.96 (d, $J_{2',6'}$ = 2.0 Hz, 1H, H-2'), 7.70 (dd, $J_{6',5'}$ = 8.8 Hz, $J_{6',2'}$ = 2.0 Hz, 1H, H-6'), 7.10 (d, $J_{5',6'}$ = 8.8 Hz, 1H, H-5').

2-((4*H*-1,2,4-Triazol-4-ylimino)methyl)-3-bromo-6-methoxyphenol (22)

White powder, Yield: 0.22 g (80%), M.p: 233-234 ˚C; ^{1}H-NMR: (400 MHz, DMSO-d_6) δ 10.63 (br.s, 1H, OH-6'), 9.23 (s, 2H, H-3, H-5), 9.11 (s, 1H, N=CH), 7.22 (d, $J_{4',5'}$ = 8.8 Hz, 1H, H-4'), 7.10 (d, $J_{5',4'}$ = 8.0 Hz, 1H, H-5'), 3.83 (s, 3H, OCH_3-5'); EI-MS: *m/z* (rel. abund. %) 297 (M^+, 9), 299 (M^++2, 6), 164 (25), 229 (70), 217 (100), 202 (67), 186 (59), 122 (42), 174 (16), 158 (22), 92 (22), 70 (37), 63 (32).

(5-Bromo-2-methoxyphenyl)-*N*-(4*H*-1,2,4-triazol-4-yl) methanimine (23)

White powder, Yield: 0.2 g (70%), m.p: 225-226 ˚C; ^{1}H-NMR: (400 MHz, DMSO-d_6) δ 9.18 (s, 2H, H-3, H-5), 9.10 (s, 1H, N=CH), 7.98 (d, $J_{6',5'}$ = 2.4 Hz, 1H, H-6'), 7.74 (dd, $J_{4',3'}$ = 8.8 Hz, $J_{4',5'}$ = 2.4 Hz, 1H, H-4'), 7.20 (d, $J_{3',4'}$ = 8.8 Hz, 1H, H-3'); EI-MS: *m/z* (rel. abund. %): 280 (M^+, 61), 282 (M^++2, 67), 199 (86), 197 (89), 169 (22), 118 (100), 91 (57), 79 (32), 76 (26).

***N*-(2-Fluoro-4-methoxybenzylidene)-4*H*-1,2,4-triazol-4-amine (24)**

White powder, Yield: 0.20 g (90%), M.p.: 183-184 ˚C; ^{1}H-NMR: (400 MHz, DMSO-d_6) δ 9.15 (s, 2H, H-3, H-5), 9.04 (s, 1H, -N=CH), 7.92 (t, $J_{3',5',6'}$ = 8.4 Hz, 1H, H-3'), 7.04 (dd, $J_{5',3'}$ = 2.4 Hz, $J_{5',6'}$ = 12.8 Hz, 1H, H-5'), 6.97 (dd, $J_{6',2'}$ = 2.0 Hz, $J_{6',5'}$ = 8.0 Hz, 1H, H-6'), 3.85 (s, 3H, -OCH_3-4'); EI-MS: *m/z* (rel. abund. %) 220 (M^+, 100), 152 (33), 138 (93), 123 (28), 109 (96), 95 (29), 75 (27).

(4-Fluoro-3-methoxyphenyl)-*N*-(4*H*-1,2,4-triazol-4-yl)methanimine (25)

White powder, Yield: 0.20 g (90%), M.p.: 118-119 ˚C; ^{1}H-NMR: (400 MHz, DMSO-d_6) δ 9.12 (s, 2H, H-3, H-5), 9.05 (s, 1H, -N=CH), 7.62 (d, $J_{6',5'}$ = 8.4 Hz, 1H, H-6'), 7.45 (d, $J_{5',6'}$ = 8.8 Hz, 2H, H-6', H-2'). EI-MS: *m/z* (rel. abund. %) 220 (M^+, 100), 150 (13), 138 (19), 109 (24), 82 (46).

1-(2-Chloro-5-nitrophenyl)-N-(4*H*-1,2,4-triazol-4 yl) methanimine (26)

White powder, Yield: 0.21 g (90%), M.p.: 185-186 ˚C; ^{1}H-NMR: (400 MHz, DMSO-d_6) δ 9.33 (s, 2H, H-3, H-5), 9.27 (s, 1H, -N=CH), 8.76 (d, $J_{6',4'}$ = 2.8 Hz, 1H, H-6'), 8.40 (dd, $J_{4',6'}$ = 2.8 Hz, $J_{4',3'}$ = 8.8 Hz, 1H, H-4'), 7.95 (d, $J_{3',4'}$ = 9.2 Hz, 1H, H-3'). EI-MS: *m/z* (rel. abund. %) 251 (M^+, 48), 253 (M^++2, 19), 164 (25), 217 (14), 216 (100), 170 (68), 123 (47).

3-((4*H*-1,2,4-Triazol-4-ylimino)methyl)-5-nitrophenol (27)

Yellow powder, Yield: 0.20 g (80%), M.p: 255-256 ˚C; ^{1}H-NMR: (400 MHz, DMSO-d_6) δ 11.36 (br.s, 1H, -OH-3'), 9.40 (s, 1H, -N=CH), 9.18 (s, 2H, H-3, H-5), 8.17 (d, $J_{3',4'}$ = 9.2 Hz, 1H, H-3'), 7.29 (d, $J_{6',4'}$ = 2.8 Hz, 1H, H-6′), 7.12 (dd, $J_{4',6'}$ = 2.4 Hz, $J_{4',3'}$ = 8.8 Hz, 1H, H-4'); EI-MS: *m/z* (rel. abund. %) 233 (M^+, 100), 216 (23), 187 (42), 164 (36), 150 (24), 134 (24), 120 (33), 107 (28), 106 (25), 70 (30), 51 (22).

3-(-(4*H*-1,2,4-Triazol-4-ylimino)methyl)pyridin-2-amine (28)

Yellow powder, Yield: 0.2 g (90%), M.p: 243-245 ˚C; ^{1}H-NMR: (400 MHz, DMSO-d_6) δ 9.15 (s, 2H, H-3, H-5), 9.13 (s, 1H, N=CH), 8.19 (dd, $J_{4',5'}$ = 5.2 Hz, $J_{4',6'}$ = 1.2 Hz, 1H, H-4'), 8.01 (d, $J_{6',NH2}$ = 7.6 Hz, 3 H, H-6', NH_2-2'), 6.92 (m, 1H, H-5'). EI-MS: *m/z* (rel. abund. %) 188 (M^+, 100), 120 (45), 119 (89), 92 (51), 79 (32), 69 (37).

***N*-(4-(Benzyloxy) benzylidene)-4*H*-1,2,4-triazol-4-amine (29)**

White powder, Yield: 0.26 g (90%), M.p: 157-159 ˚C; ^{1}H-NMR: (400 MHz, DMSO-d_6) δ 9.07 (s, 2H, H-3, H-5), 8.98 (s, 1H, -N=CH), 7.81 (d, $J_{2',6'}$ = $J_{6',2'}$ = 8.8 Hz, 2H, H-2', H-6'), 7.47 (d, $J_{2'',6''}$ = 7.2 Hz, 2H, H-2", H-6"), 7.42 (t, $J_{3'',5''}$ = 7.2 Hz, 2H, H-3", H-5"), 7.35 (m, 1H, H-4"), 7.19 (d,

$J_{3',5'}$ = 8.8 Hz, 2H, H-3', H-5'), 5.19 (s, 2H, H-OCH_2); EI-MS: *m/z* (rel. abund. %): 278 (M^+, 60), 91 (100), 65 (16).

***N*-(3-(Benzyloxy)-4-methoxybenzylidene)-4*H*-1,2,4-triazol-4-amine (30)**

White powder, Yield: 0.3 g (95%), M.p: 165-166 ˚C; ^{1}H-NMR: (400 MHz, DMSO-d_6) δ 9.07 (s, 2H, H-3, H-5), 8.95 (s, 1H, N=CH), 7.54 (s, 1H, H-2'), 7.53 ($J_{2'',6''}$ = 7.2 Hz, 2H, H-2'', H-6''), 7.46 (t, $J_{3'',4'',5''}$ = 6.8 Hz, 3H, H-3'', H-4'', H-5''), 7.35 (d, $J_{6',2'}$ = 7.2 Hz, 1H, H-6'), 7.17 (d, $J_{5',6'}$ = 7.2 Hz, 1H, H-5'), 5.14 (s, 2H, OCH_2), 3.85 (s, 3H, -OCH_3- 4'); EI-MS: *m/z* (rel. abund. %): 308 (M^+, 23), 307 (29), 279 (14), 160 (54), 89 (76), 77 (86), 164 (68), 103 (32), 91 (30), 51 (85).

***N*-(Anthracen-9-ylmethylene)-4*H*-1,2,4-triazol-4-amine (31)**

Light green powder, Yield: 0.21 g (96%), M.p: 239-240 ˚C; ^{1}H-NMR: (400 MHz, DMSO-d_6)δ 10.14 (s, 1H, -N=CH), 9.38 (s, 2H, H-3, H-5), 8.87 (s, 1H, H-6'), 8.77 (d, $J_{2',3',5',4'}$ = 8.8 Hz, 2H, H-2', H-5'), 8.21 (d, $J_{7',8',9',10'}$ = 8.0 Hz, 2H, H-7', H-10'), 7.69 (m, 4H, H- 3', H-4', H-8', H-9'); EI-MS: *m/z* (rel. abund. %): 272 (M^+, 58), 205 (100), 177 (34), 101 (6), 88 (34), 69 (11).

(Pyren-2-yl)-*N*-(4*H*-1,2,4-triazol-4-yl)methanimine (32)

Yellow powder, Yield: 0.23 g (78%), M.p.: 246-247 ˚C; ^{1}H-NMR: (400 MHz, MeOD-d_4) δ 10.05 (s, 1H, N=CH), 9.38 (d, 2H, H-3, H-5), 9.07 (d, $J_{1',2'}$ = 9.2 Hz, 1H, H-1'), 8.72 (d, $J_{2',1'}$ = 8.4 Hz, 1H, H-2'), 8.46 (m, 4H, H-3', H-4', H-8', H-9'), 8.38 (d, $J_{7',6'}$ = 8.8 Hz, 1H, H-7'), 8.29 (d, $J_{5',6'}$ = 9.2 Hz, 1H, H-5'), 8.19 (t, $J_{6',5',7'}$ = 7.6 Hz, 1H-6'). EI-MS: *m/z* (rel. abund. %) 296 (M^+, 100), 297 (M^++ 1, 66), 240 (34), 227 (90), 213 (68), 201 (76), 107 (53).

(1*H*-Indol-2-yl)-*N*-(4*H*-1,2,4-triazol-4-yl) methanimine (33)

Pink powder, Yield: 0.3 g (91%), M.p: 304-306 ˚C; ^{1}H-NMR: (400 MHz, DMSO-d_6) δ 11.98 (br.s, 1H, NH-3'), 9.06 (s, 1H, -N=CH), 9.03 (s, 2H, H-3, H-5), 8.18 (d, $J_{4',5'}$ = 7.6 Hz, 1H, H-4'), 8.00 (s, 1H, H-2'), 7.52 (d, $J_{7',6',5'}$ = 8.0 Hz, 1H, H-7'), 7.28 (m, 2H, H-6', H-5'); EI-MS: *m/z* (rel. abund. %) 211 (M^+, 100), 142 (88), 129 (77), 64 (11).

Acknowledgement: The authors are thankful to Pakistan Academy of Sciences for providing financial support to project No. 5-9/PAS/440.

References:

1. Zhou, C. H., and Wang, Y. (2012). Recent researches in triazole compounds as medicinal drugs. *Current Medicinal Chemistry*, 19(2), 239-280.

2. Stefanska, J., Szulczyk, D., Koziol, A. E., Miroslaw, B., Kedzierska, E., Fidecka, S.,and Struga, M. (2012). Disubstituted thiourea derivatives and their activity on CNS: Synthesis and biological evaluation. *European Journal of Medicinal Chemistry*, 55, 205-213.
3. Mi, J., Wu, J., and Zhou, C. (2008). Progress in anti-tumor agents: triazoles. *West China Journal of Pharmaceutical Sciences*, 23, 84-86.
4. Jia-li, M., and Cheng-he, Z. (2007). and Bai Xue2 (1 School of Pharmaceutical Sciences, Chongqing Medical University, Chongqing 400016; 2 School of Chemistry and Chemical Engineering, Southwest University, Chongqing 400715); Advances in triazole antimicrobial agents [J]. *Chinese Journal of Antibiotics*, *10*.
5. Wang, Y., and Zhou, C. (2011). Recent advances in the researches of triazole compounds as medicinal drugs. *Scientia Sinica Chimica*, 41(9) 1429-1456.
6. Amtul, Z., Rasheed, M., Choudhary, M. I., Rosanna, S., and Khan, K. M. (2004). Kinetics of novel competitive inhibitors of urease enzymes by a focused library of oxadiazoles/thiadiazoles and triazoles. *Biochemical and Biophysical Research Communications*, *319*(3), 1053-1063.
7. Kucukguzel, S. G., and Cikla-Suzgun, P. (2015). Recent advances bioactive 1,2,4-triazole-3-thiones. *European Journal of Medicinal Chemistry*, 97, 830-870.
8. Kuang, J., Chen, B. and Ma, S. (2014). Copper-mediated efficient three-component synthesis of 1,2,4-triazoles from amines and nitriles. *Organic Chemistry Frontiers*, 1(2), 186-189.
9. Goldenberg, R. and Punthakee, Z. (2013). Definition, classification and diagnosis of diabetes, prediabetes and metabolic syndrome. *Canadian Journal of Diabetes*, 37, S8-S11.
10. Shim, Y. J., Doo, H. K., Ahn, S. Y., Kim, Y. S., Seong, J. K., Park, I. S., and Min, B. H. (2003). Inhibitory effect of aqueous extract from the gall of Rhus chinensis on *α*-glucosidase activity and postprandial blood glucose. *Journal of Ethnopharmacology*, *85*(2-3), 283-287.
11. Samad, A. H., Willing, T. S. T., Alberti, K. G. M., and Taylor, R. (1988). Effects of BAYm 1099, new *α*-glucosidase inhibitor, on acute metabolic responses and metabolic control in NIDDM over 1 mo. *Diabetes Care*, *11*(4), 337-344.
12. Asano, N. (2003). Glycosidase inhibitors: update and perspectives on practical use. *Glycobiology*, 13(10), 93R-104R.

13. Johnson, A. B. and Taylor, R. (1996). Does suppression of postprandial blood glucose excursions by the *α*-glucosidase inhibitor miglitol improve insulin sensitivity in diet-treated type II diabetic patients. *Diabetes Care*, 19(6), 559-563.

14. Puls, W., Keup, U., Krause, H. P., Thomas, G., and Hoffmeister, F. (1977). Glucosidase inhibition. *Naturwissenschaften*, *64*(10), 536-537.

15. Khan, K. M., Rahim, F., Wadood, A., Kosar, N., Taha, M., Lalani, S., and Khan, M. (2014). Synthesis and molecular docking studies of potent *α*-glucosidase inhibitors based on biscoumarin skeleton. *European Journal of Medicinal Chemistry*, *81*, 245-252.

16. Joshi, S. R., Standl, E., Tong, N., Shah, P., Kalra, S., and Rathod, R. (2015). Therapeutic potential of *α*-glucosidase inhibitors in type 2 diabetes mellitus: an evidence-based review. *Expert Opinion on Pharmacotherapy*, *16*(13), 1959-1981.

17. Ranilla, L. G., Kwon, Y. I., Apostolidis, E., and Shetty, K. (2010). Phenolic compounds, antioxidant activity and *in vitro* inhibitory potential against key enzymes relevant for hyperglycemia and hypertension of commonly used medicinal plants, herbs and spices in Latin America. *Bioresource Technology*, *101*(12), 4676-4689.

18. Toeller, M. (1994). *α*-Glucosidase inhibitors in diabetes: efficacy in NIDDM subjects. *European Journal of Clinical Investigation*, 24(S3), 31-35.

19. Taha, M., Javid, M. T., Imran, S., Selvaraj, M., Chigurupati, S., Ullah, H., and Khan, K. M. (2017). Synthesis and study of the *α*-amylase inhibitory potential of thiadiazole quinoline derivatives. *Bioorganic Chemistry*, 74, 179-186.

20. Asgher, M., Asad, M. J., Rahman, S. U., and Legge, R. L. (2007). A thermostable *α*-amylase from a moderately thermophilic *Bacillus subtilis* strain for starch processing. *Journal of Food Engineering*, 79(3), 950-955.

21. Gunawan-Puteri, M. D., Kato, E., and Kawabata, J. (2012). *α*-Amylase inhibitors from an Indonesian medicinal herb, *Phyllanthus urinaria. Journal of the Science of Food and Agriculture*, *92*(3), 606-609.

22. Akhtar, T., Hameed, S., Khan, K. M., Khan, A., and Choudhary, M. I. (2010). Design, synthesis, and urease inhibition studies of some 1, 3, 4-oxadiazoles and 1, 2, 4-triazoles derived from mandelic acid. *Journal of Enzyme Inhibition and Medicinal Chemistry*, *25*(4), 572-576.

23. Akhtar, T., Hameed, S., Al-Masoudi, N. A., and Khan, K. M. (2007). Synthesis and anti-HIV activity of new chiral 1,2,4-triazoles and 1,3,4-thiadiazoles. *Heteroatom Chemistry: An International Journal of Main Group Elements*, *18*(3), 316-322.

24. Hameed, S., Kanwal., Seraj, F., Rafique, R., Chigurupati, S., Wadood, A., Rehman, A. U., Venugopal, V., Salar, U., Taha, M.,and Khan, K. M. (2019). Synthesis of benzotriazoles derivatives and their dual potential as *α*-amylase and *α*-glucosidase inhibitors *in vitro:* Structure-activity relationship, molecular docking, and kinetic studies. *European Journal of Medicinal Chemistry*, *183*, 111677

25 Rafique, R., Khan, K. M., Arisha., Kanwal., Chigurupati, S., Wadood, A., Rehman, A. U., Karunanidhi, A., Hameed, S., Taha, M and Al-Rashida, M. (2019). Synthesis of new indazole based dual inhibitors of *α*-glucosidase and *α*-amylase enzymes, their *in vitro*, *in silico* and kinetics studies. *Bioorganic Chemistry*, 103195.

26. Ali, F., Khan, K. M., Salar, U., Taha, M., Ismail, N. H., Wadood, A., and Perveen, S. (2017). Hydrazinyl arylthiazole based pyridine scaffolds: Synthesis, structural characterization, in vitro *α*-glucosidase inhibitory activity, and *in silico* studies. *European Journal of Medicinal Chemistry*, *138*, 255-272.

27. Salar, U., Khan, K. M., Chigurupati, S., Taha, M., Wadood, A., Vijayabalan, S., and Perveen, S. (2017). New hybrid hydrazinyl thiazole substituted chromones: as potential *α*-amylase inhibitors and radical (DPPH and ABTS) scavengers. *Scientific Reports*, *7*(1), 16980.

28. Khan, K. M., Qurban, S., Salar, U., Taha, M., Hussain, S., Perveen, S., and Wadood, A. (2016). Synthesis, *in vitro α*-glucosidase inhibitory activity and molecular docking studies of new thiazole derivatives. *Bioorganic Chemistry*, *68*, 245-258.

29. Yousuf, S., Khan, K. M., Salar, U., Chigurupati, S., Muhammad, M. T., Wadood, A., and Perveen, S. (2018). 2′-Aryl and 4′-arylidene substituted pyrazolones: As potential *α*-amylase inhibitors.*European Journal of Medicinal Chemistry*,*159*, 47-58.

30. Ramirez-Escudero, M., Gimeno-Perez, M., Gonzalez, B., Linde, D., Merdzo, Z., Fernandez-Lobato, M., and Sanz-Aparicio, J. (2016). Structural analysis of *β*-fructofuranosidase from Xanthophyllomyces dendrorhous reveals unique features and the crucial role of *N*-glycosylation in oligomerization and activity. *Journal of Biological Chemistry*, *291*(13), 6843-6857.

31. Molecular Operating Environment (MOE), 2016.08; Chemical Computing Group Inc., 1010 Sherbrooke St. West, Suite #910, Montreal, QC, Canada, H3A 2R7, 2016.

32. Carreiro, E. P., Louro, P., Adriano, G., Guedes, R. A., Vannuchi, N., Costa, A. R., .and Burke, A. J. (2014). 3-Hydroxypyrrolidine and (3, 4)-dihydroxypyrrolidine derivatives: Inhibition of rat intestinal *α*-glucosidase. *Bioorganic Chemistry*, *54*, 81-88.

Graphical abstract

Syntheses, *in vitro* α-amylase and α-glucosidase dual inhibitory activities of 4-amino-1,2,4-triazole derivatives their molecular docking and kinetic studies

Emmanuel Oloruntoba Yeye,[a,b] Kanwal,[a] Khalid Mohammed Khan, [a,c] Sridevi Chigurupati,[d] Abdul Wadood,[e] Ashfaq Ur Rehman,[e] Shahnaz Perveen,[f] Mari Kannan Maharajan,[g] Shahbaz Shamim,[a] Shehryar Hameed,[a] Sherifat A. Aboaba,[b] Muhammad Taha[c]

[a]*H. E. J. Research Institute of Chemistry, International Center for Chemical and Biological Sciences, University of Karachi, Karachi-75270, Pakistan*

[b]*Organic Unit, Chemistry Department, University of Ibadan, Nigeria*

[c]*Department of Clinical Pharmacy, Institute for Research and Medical Consultations (IRMC), Imam Abdulrahman Bin Faisal University, P.O. Box 1982, Dammam 31441, Saudi Arabia*

[d]*Department of Medicinal Chemistry and Pharmacognosy, Faculty of Pharmacy, Qassim University, Buraidah 52571, Kingdom of Saudi Arabia*

[e]*Department of Biochemistry, Computational Medicinal Chemistry Laboratory, UCSS, Abdul Wali Khan University, Mardan, Pakistan*

[f]*PCSIR Laboratories Complex, Karachi, Shahra-e-Dr. Salimuzzaman Siddiqui, Karachi-75280, Pakistan*

[g]*School of Pharmacy, International Medical University, Kuala Lumpur, 57000, Malaysia*

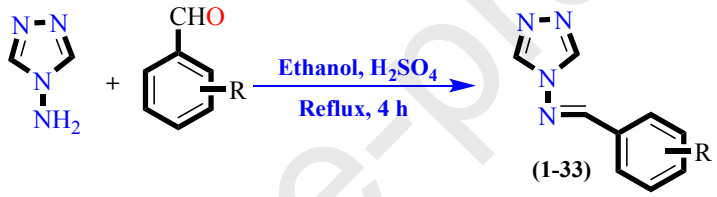

Scheme-1: Synthesis of Schiff base derivatives of 4-amino-1,2,4-triazole **1-33**.

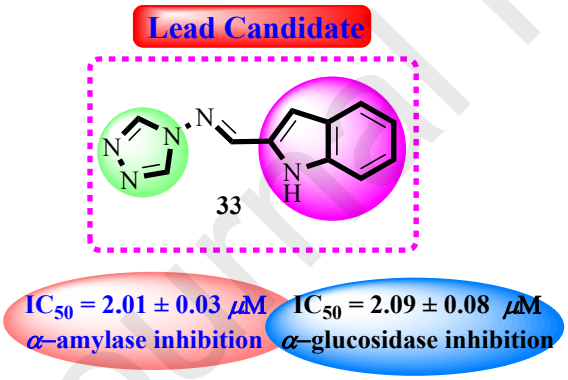

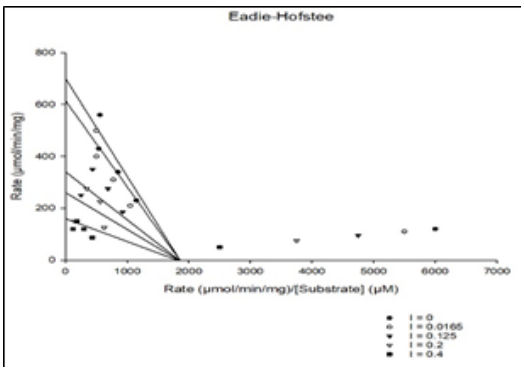

Figure-13:C) Hanes-Woolf plot of compound **33** at different concentration of [S] Vs [S]/Rate in the different concentration of mixed-type inhibitor (α-amylase)

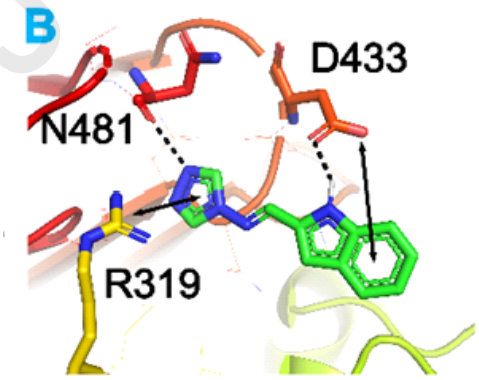

Figure-15: (B) The binding mode of the most potent compound **33** (α-amylase)

Highlights

- Schiff bases of 4-amino-1,2,4-triazole were synthesized and evaluated for their *in vitro* anti hyperglycemic potential.
- Kinetics confirmed that both enzymes are inhibited via different modes.
- The binding interactions of molecules within the active site of enzyme was confirmed through molecular docking studies.

Declaration of interests

☒ The authors declare that they have no known competing financial interests or personal relationships that could have appeared to influence the work reported in this paper.

☐The authors declare the following financial interests/personal relationships which may be considered as potential competing interests: